

*Kinematical Model
of the
Human Elbow*

*Research Report of Joanne Minekus
Sub-faculty of Biology, Leiden University
Research done at the Man Machine Group,
Technical University of Delft
and at the Department of Anatomy and Embryology,
Leiden University*

*Supervisors : C.W. Spoor
F.C.T. Van der Helm*

Date : 28 July 1997

APPENDICI

Appendix A : Parameter file

Appendix B : Input file

Appendix C : Tables of measured parameters

Appendix D : Figures of flexion

Appendix E : Figures of pronation

Appendix F : Figures of the effect of pronation on flexion

Appendix G : Figures of the effect of flexion on pronation

SUMMARY

A complete parameter set of elbow muscles has been measured. The dataset consists of bony contours, rotation axis and centres, muscle attachment sites, muscle mass and PCSA, muscle length, fibre length and sarcomere lengths. A complete parameterset of the shoulder muscles has already been measured of the same cadaver (Klein Breteler, 1996). These two parameter sets combined give an unique shoulder/elbow model.

With this dataset the change in muscle length and moment arm during flexion and pronation is calculated by the Dutch shoulder model (Jonker, 1988; Van der Helm, 1988; Pronk, 1989; Van der Helm and Pronk, 1989; Van der Helm et al, 1992; Van der Helm 1994 a,b; Werff, 1977; Werff and Jonker, 1983). From the muscle length the sarcomere lengths can be calculated. The relative force depends on the sarcomere length. The relative force multiplied with the PCSA and a constant value for muscle stress gives the maximum force. The maximum moment during flexion is calculated by multiplying the maximum force with the moment arm.

Figure 7 and 8 show the change of maximal moments during flexion and pronation. The biceps, the brachialis, the brachioradialis and the pronator teres are the flexors. The triceps and the anconeus are the extensors. The pronator teres and the pronator quadratus are the pronators. The supinators are the biceps and the supinator. The brachioradialis is a supinator when the forearm is pronated and a pronator when the forearm is supinated.

The moment arms of the flexors are similar to those known from literature (figure 9; Murray et al, 1995). The triceps has a rather small moment arm. For the other muscles not much research work has been done to the moment arms.

The maximum moments are rather small compared to the measured maximum moments at living persons. The maximum moments are comparable to those calculated with other models (An et al, 1989; Kleweno, 1985). The transposition factor from PCSA to muscle strength is disputable.

Chapter 1 INTRODUCTION

1.1 The shoulder model

At the Delft University of Technology, a dynamical model of the human shoulder has been developed, using the finite element method (Jonker, 1988; Van der Helm, 1988; Pronk, 1989; Van der Helm and Pronk, 1989; Van der Helm et al, 1992; Van der Helm 1994 a,b; Werff, 1977; Werff and Jonker, 1983). In this model morphological structures are represented by elements whose dynamical behaviours are well known. The complex equation of motion for the mechanism can be derived by connecting the elements.

The shoulder consists of four bones: the thorax, the scapula, the clavicle and the humerus. The original shoulder model is expanded with the forearm, consisting of the ulna, the radius and the hand (figure 1). The incisura jugularis is the origin. The complete model has 17 degrees of freedom:

The incisura jugularis	: three translation vectors
The thorax	: three rotational vectors
The scapula and clavicle	: three translation vectors
The humerus	: abduction, anteflexion and rotation
The elbow	: flexion
The fore-arm	: pronation
The hand	: three rotation vectors

In this model the bones are represented as a single rigid MNODE element. Mass and external forces are coupled to these MNODE's. Joints are defined by a midpoint (two MNODE's) and a rotation axis (HINGE element). The spherical joints are modelled as three orthogonal HINGE elements. Two SURFACE elements represent the scapulothoracic gliding plane. A muscle is modelled by one or more active TRUSS or CURVE TRUSS elements, while the ligaments are modelled by passive TRUSS elements (Van der Helm 1994 a,b).

The input for the simulations is the position, velocity and acceleration of bony landmarks and the euler angles of the joints. Bony landmarks are points that can easily be measured on the bones of living persons (figure 1). The output is the length and the

moment arm of all muscles. By optimising the minimum muscle stress, the model calculates the force and moment of each individual muscle elements.

For the model, datasets of morphological structures are measured from different cadavers. Because of the morphological difference between cadavers, the results can not be averaged. This results in different morphological datasets.

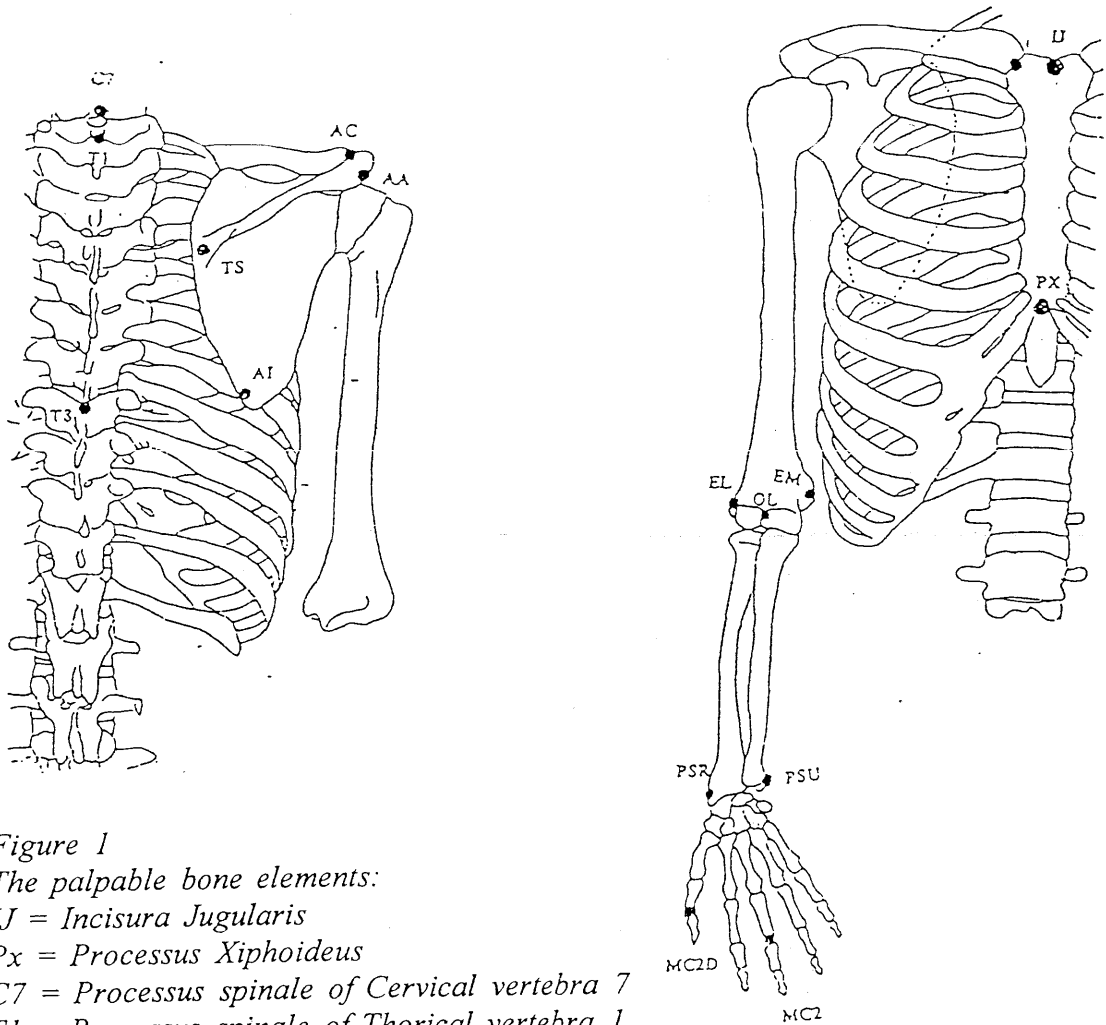


Figure 1

The palpable bone elements:

IJ = Incisura Jugularis

Px = Processus Xiphoideus

C7 = Processus spinale of Cervical vertebra 7

T1 = Processus spinale of Thorical vertebra 1

T8 = Processus spinale of Thorical vertebra 8

AC = Acromioclavicular joint

AI = Angulus Inferior

AA = Angulus Acromialis

TS = Trigonum Spinae

EL = Epicondylus Lateralis

EM = Epicondylus Medialis

PSU = Processus Styloideus Ulnae

PSR = Processus Styloideus Radii

MC2 = Articulationes interphalangeae manus 2

MC2D = Articulationes interphalangeae of the thumb

OL = Olecranon

There is one complete shoulder muscle parameter set (Klein Breteler, 1996). This parameterset includes geometric parameters, the PCSA and the sarcomere length. Muscles with large attachment sides can have separate functions for different muscle parts. Therefore the muscles are divided in several parts. For all muscle parts the optical estimated centroid of the origin and insertion places are measured. Also bony contours and rotation centres are measured.

The Physiological Cross Sectional Area (PCSA) is an indication of the maximum muscle strength (Weijjs and Hillen, 1985). There is a large variation in PCSA's between subjects. The PCSA depends on the age and the health of a subject.

A muscle fibre consists of sarcomeres. A sarcomere consists of two filaments: actin and myosin which are connected by cross bridges. During contractions the filaments slide along each other. The amount of force a sarcomere can deliver, depends on the amount of overlap between the actin and myosin filaments (Bagi et al, 1986; Huxley, 1954; Huxley, 1957). Figure 2 shows the force/length relation of a sarcomere. This relationship is used in the shoulder model.

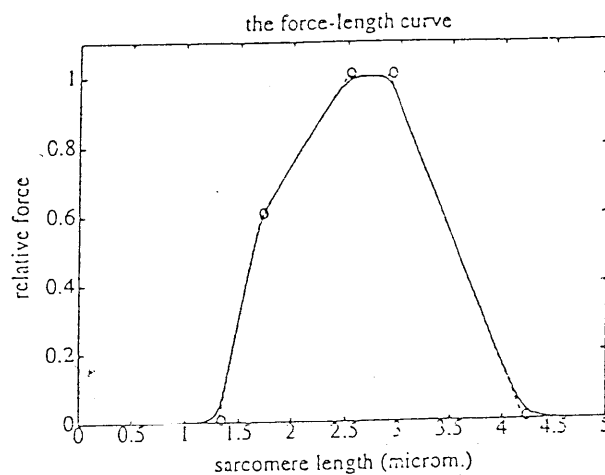


Figure 2
The force length relation of sarcomeres used in the model.

1.2 The elbow and the forearm

A human elbow consists of three bones: the humerus, the ulna and the radius. The elbow has two joints: the humero-ulnar and humero-radial joint and has one degree of freedom: flexion. During flexion the ulna and radius move towards the humerus. The humero-ulnar joint is the most important joint in this movement.

The forearm consists of the ulna and radius with are connected by the proximal and distal ulno-radial joint. There is one degree of freedom: pronation. During pronation the radius and ulna rotate around each other.

In the model the elbow and forearm are represented by two hinge joints, one for flexion and one for pronation. The axes of the two joints are not orthogonal. During flexion the humerus is fixed and the forearm rotates around the humerus. The ulna is fixed by pronation and the radius rotates.

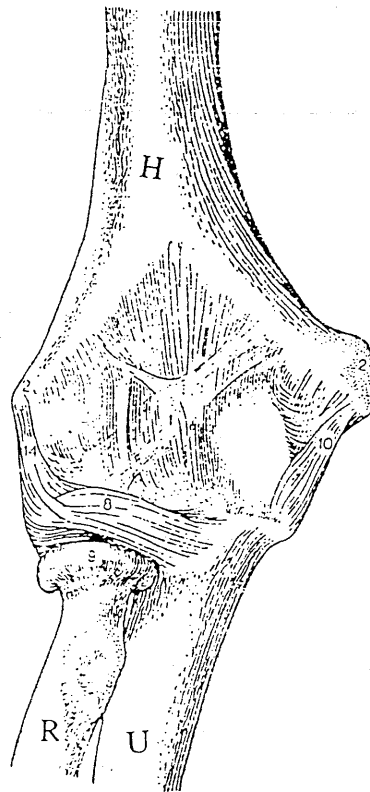


Figure 3
The elbow joint
Dorsal view
H Humerus
U Ulna
R Radius
2 epicondicii
8 ligamentum radiale
10 ligamentum collaterale ulnae
14 ligamentum collaterale radii

The movement of the elbow is limited because of the shape of the joint surfaces and because of the ligaments (figure 3). The articular surfaces of the joints are curved. Because of these curves translation of the forearm is not possible. The humerus and the ulna and the humerus and radius are connected by two important ligaments: ligamentum collaterale ulnae and ligamentum collaterale radii. In an extended elbow parts of these ligaments are taut. During flexion other parts of these ligaments become taut. Taut elements restrict the movement. Not only the ligaments, but also the muscle mass limits flexion. The muscle bellies of the fore and upper arm reaches each other during flexion. The radius and the ulna are linked up by several ligaments. The membrana interossea connects the whole length of the two bones. The ligamentum annulare radii lays around the radius head and is connected on both sides to the ulna. The radius can rotate within this ligament.

Sixteen muscles cross the elbow joint. The muscles used for the four elbow movements are (An, 1981; Fick, 1910, Murray, 1995):

1. The flexors: The biceps, the brachialis and the brachioradialis are the most important flexors. Other flexors are the extensor carpi radialis brevis and longus, the flexor carpi radialis, the palmaris longus and the pronator teres.
2. The extensors: The triceps and the anconeus
3. The supinators: The supinator, the biceps and the brachioradialis. The brachioradialis is only a supinator when the hand is pronated.
4. The pronators: The pronator teres, the pronator quadratus, the brachioradialis, the extensor carpi radialis longus and the palmaris longus. The brachioradialis is only a pronator when the hand is supinated.

The eight main muscles are built in this model: the biceps, the triceps, the brachioradialis, the brachialis, the anconeus, the pronator teres, the pronator quadratus and the supinator. The other muscles have their main influence on the hand and finger movement and have just a small influence on elbow flexion or pronation.

The elbow helps in positioning the hand and it transmits forces from the hand to the shoulder. During daily activities, the human elbow has to transmit forces equal to approximately a third of the body weight. By picking up objects the elbow transmits forces 5-7 times the weight of the object (Souter, 1981). Those forces are caused by large moments on the elbow.

The maximum moment of a muscle depends on the PCSA and the moment arm of that muscle. Most studies measure either the moment arms (Amis et al, 1979; An et al, 1981; An et al, 1984; Crowninshield & Brand, 1981; Murray, 1995; Winter & Kleweno, 1993; van Zuylen et al, 1988) or the maximal moment (Chauffin & Anderson, 1984; Darcus, 1951; Jorgenson & Bankov, 1971; MacGarvey et al, 1984; Larson, 1969; Salter & Darcus, 1957; Singh & Karpovich, 1968; Winters & Stark, 1985; Winters et al, 1988). A few model studies (An et al, 1989; Kleweno, 1987) are done to both muscle force and moment arms.

The model of An et al (1989) includes also a force/length relationship. They define an index of architecture as the mean fibre length divided by the muscle belly at the muscle optimal length. The relative force depends mathematical on this index. They did not measure the sarcomere length.

There is a large variation in maximum moments between subjects. Males have larger muscle moments than females (Winters & Kleweno, 1993). The maximum flexion moment depends on the degree of pronation of the forearm and on the position of the shoulder. When the hand is supinated the maximum flexion moment is larger. By increase of shoulder flexion the top of the flexion moment is at an increased elbow flexion angle (Winter & Kleweno, 1993). Most elbow muscles are biarticulair. During movement of one of the joints the muscle length and moment arm may change. A change muscle length causes a different sarcomere length and so a different relative muscle force. Change in either the moment arm or muscle force result in a different moment of the muscle.

1.3 Aim of this study

To learn more about the movement of the arm, a complete muscle model of the arm is needed. Such a model can be used for several purposes. The faculty of Human Movement Science of the Free University of Amsterdam is interested in wheelchair movements. They can use a complete arm model for predicting arm forces in wheelchair movements.

A complete parameter set of the shoulder muscles is measured by Klein Breteler (1996). There is a large variation in muscle attachments between specimen. Therefore the elbow measurements are done on the same cadaver as the shoulder measurements. As a result a complete shoulder/elbow model is obtained in this study. There are a few shoulder muscle models or elbow muscle models but a combined shoulder/elbow model is unique. Also unique is the inclusion of the sarcomere length as a measure of the relative force of the muscle.

From these measurements the moment arms, the maximum forces and moments are calculated for different flexion and pronation angles. The influence of pronation on flexion is also studied. In the discussion the results of this study are compared with other model studies and with measurements at test persons.

Chapter 2 MATERIALS AND METHODS

2.1 Dissection

For the measurements the right arm of a 57-year old male specimen is used. The dissection and measurements are made at the Anatomic Laboratory of the Medical Faculty of the Leiden University. The same specimen is used for shoulder measurements (Klein Breteler, 1996). Steel screws are driven in the specimen and are used to determine the local co-ordinate system and to transpose the bones to the global co-ordinate system.

Some muscles have large attachment sites. Different parts of the muscle can have different functions. Therefore the muscles are divided in multiple parts. The parts are treated as separate muscles. The division is based on several facts:

- Place of attachment: Some muscles have different origin or insertion places.
- Tendon plate: A muscle can have different tendon plates. Different tendons can be attached to different bones.
- Gliding planes in muscles: Some muscles have clear gliding planes between the muscle parts.
- Muscle fibre length. The fibre length can vary within a muscle.

When possible the muscles are divided in situ. The divided muscles are dissected from the specimen. The estimated mean attachment site at the muscle is marked by sewing a number onto the muscle. A number nailed into the bone marks the corresponding place at the bone. The bone is too hard to hammer, so a hole had to be drilled first. Some muscles were difficult to divide in situ. Before dissecting, the surroundings of these muscle were marked at the bone and at the muscle. Thereafter the muscle is dissected from the specimen and divided in several parts. Of each muscle part the mean attachment site is estimated. The muscle parts are returned to the bone with help of the markers. The corresponding mean attachment sites at the bone are marked.

All muscles crossing the elbow leading to the hand are cut at the level of the retinaculum flexorum and extensorum. The muscles which are not used for this model are still in the arm or they are prepared and handled just like the muscles in the model.

2.2 The geometric parameters

The geometric parameters are:

- Origin and insertion of the muscles.
- Origin and insertion of the ligaments.
- The shape and position of the bony contours.
- The rotation centres of the joints.
- The position of well defined bony landmarks.

The geometric parameters of the shoulder model have been measured with the palpator (figure 4). The palpator is an open chain, which consists of four links of 20 cm length each. The links are connected by hinge joints with axes perpendicular to each other. After measuring the rotations of the joints, a computer programme calculates the tip position co-ordinates of the palpator. The standard error is 0.96 mm for each co-ordinate and 1.43 mm for an absolute distance (Pronk & Van der Helm, 1991). In the bones 4 to 5 orientation screws are driven. Before dissecting, the positions of all these screws are measured. From those measurements the global co-ordinate system is derived. By later measurements the screws are measured again. With help of these screws, the measurements can be transformed to the global co-ordinate system.

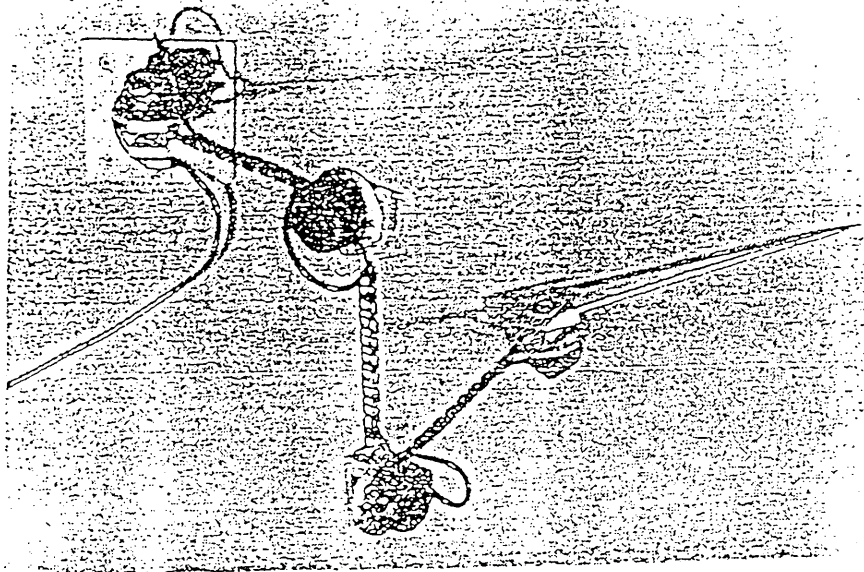


Figure 4
The palpator

The shapes of the joints and bony contours determining the muscle pathway are measured. These structures are represented by geometric shapes in the model. The parameters of these shapes are estimated from the measurements by using a least squares error criterion. The thickness of the muscles are neglected.

The flexion axis is calculated with help of screw axis. The humerus is fixed to a steel frame. The ulna and radius are fixed to each other. The orientation screws of the humerus, ulna and radius are measured with the palpator for six different flexion angles. The rotation matrix, the rotation axis and translation vector between each pair of measurements are calculated (Veldpaus et al, 1988). The averaged rotation axis is the flexion axis used in the model. For the pronation axis, the radius is fixed to the frame and the radius and ulna orientation screws are measured for five different pronation angles. From these measurements the pronation axis is calculated.

2.3 The muscle parameters

For each muscle part, the total muscle length between the markers is measured. Three muscle fibre bundles of about 3 mm diameter are dissected from each muscle part. The length of each fibre is measured. The total muscle length (l_m) minus the mean fibre length (l_f) gives the tendon length (l_t).

$$l_t = l_m - l_f \quad (1)$$

A sarcomere is the smallest functional unit of a muscle. A sarcomere consists of an A-line with the thick myosin filaments and an I-line with the thinner actin filaments. A small part of a muscle can be regarded as a diffracting lattice. The A-lines behave as the bars and the I-lines as the slits. When a laser bundle passes through the fibre, the light will be diffracted. At a fixed distance of the fibre, a calibrated scale is placed. The sarcomere length is read from the scale (figure 5).

Of each prepared muscle fibre, the sarcomere length is determined. The sarcomere length varies over the muscle fibre. The variation is about 0.20 μm . Therefore the sarcomere

length is determined at 4 to 15 places spread over each muscle fibre. The number of measurements depended on the fibre length. All measurements of each muscle part are averaged as the mean sarcomere length (l_s) of that muscle part.

Sample preparation does not influence the sarcomere length. After being pulled apart, the sarcomere length shrinks to its starting length (Klein Breteler, 1995).

The optimal sarcomere length is $2.7 \mu\text{m}$ (Walker & Schrodt, 1974). The number of sarcomeres (n_s) is calculated by dividing the measured fibre length by the mean sarcomere length (l_s). The optimal fibre length (l_0) is calculated by multiplying the number of sarcomeres with the optimal sarcomere length.

$$n_s = l_f / l_s \quad (2)$$

$$l_0 = l_f * 2.7 / l_s \quad (3)$$

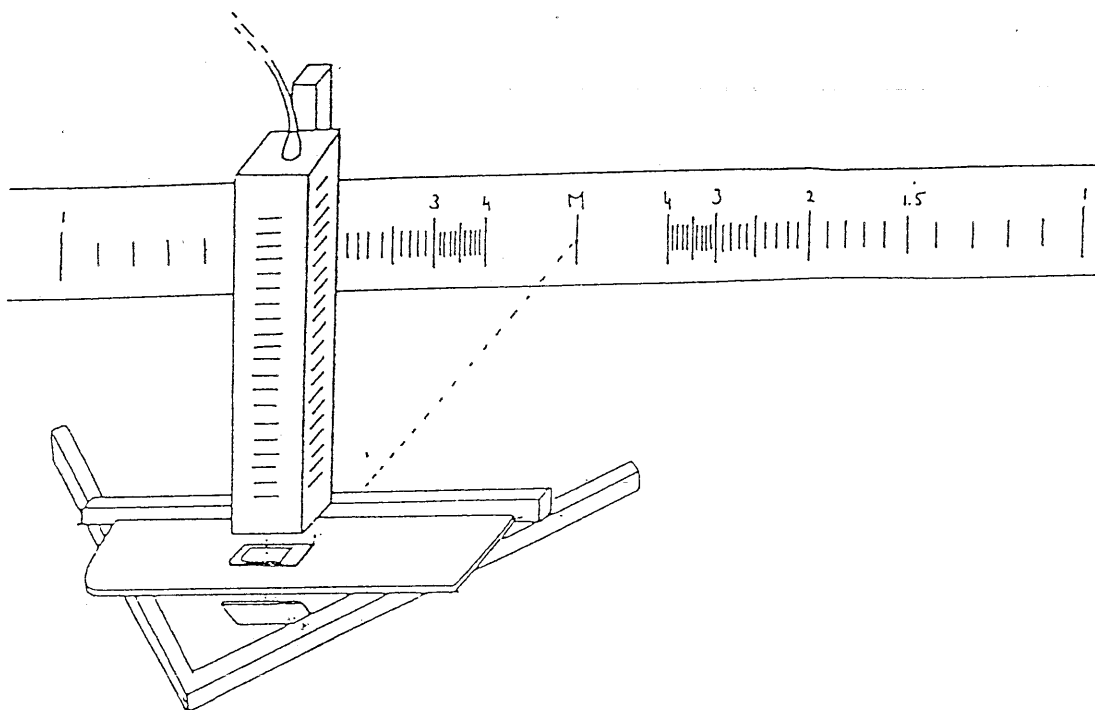


Figure 5 The laser diffraction setup.

A laser bundle is reflected in a 45 degrees mirror to the scale. In the bundle, a sample is placed at a microscope slide. The sample refracts the light. The diffraction angle depends on the sarcomere length, which can be read at the scale.

The soaked mass of all muscle bellies without the tendons is measured. The specific density (δ) of muscle tissue is 1.0576 g cm^{-3} (measured by Klein Breteler 1996). The volume of the muscle is the mass divided by the specific density. The volume of a muscle remains constant during contraction. The volume divided by the optimal fibre length gives the PCSA.

$$\text{PCSA} = M / (\delta * l_0) \quad (4)$$

2.4 Model simulation

The model simulations are done in the Man Machine group of the department of Mechanical Engineering and Marine Technology at the Delft University of Technology. For the simulations a Silicon Graphics computer is used. In the Delft University a program SPACAR has been developed by the group Technical Mechanics of the department Mechanical Engineering and Marine Technology. SPACAR is written in FORTRAN 77. It is a finite element method used for dynamic analysis of flexible mechanisms and is used to build the shoulder model (Jonker, 1988; Van der Helm, 1988; Pronk, 1989; Van der Helm and Pronk, 1989; Van der Helm et al, 1992; Van der Helm 1994a,b; Werff, 1977; Werff and Jonker, 1983). The results of the model simulations can be imported in Matlab for further calculations.

The morphology of the shoulder and the elbow are placed in a parameter file. The morphology includes the places of origin and insertion, the bony contours, the rotation axes, the palpable bony landmarks and the PCSA. The parameter file is given in appendix A. At healthy test persons the positions of the palpable bone elements have been measured. These results can be used as input for the model simulations. The input file used for this study is given in appendix B. The input file is a combination of the positions of bony landmarks and euler angles of the joints.

The model has 17 degrees of freedom. There are six translation vectors: three at the incisura jugularis and three at the scapula/clavicula. The other eleven degrees of freedom are euler angles: three for the thorax, three for the humerus, one for the elbow, one for the forearm and three for the hand. In this study only the angles of the elbow and forearm change, the other degrees of freedom are constant.

At the beginning of a simulation, the model checks all mechanical constraints for the given position. Thereafter the model calculates the geometric parameters for the arm in all given positions. These parameters are the insertions and origins of all muscles, the positions of the joints, bony contours and ligaments and the lengths and moment arms of all muscle parts. Finally, the model calculates the muscle forces and moments by optimising the minimum force. As output the model gives matlab files with the calculated parameters.

For this study, only the muscle lengths and moment arms (ma) calculated by the model are used. From the muscle length, the fibre length and sarcomere length are calculated.

$$l_f = l_m - l_t \quad (5)$$

$$l_s = l_f / n_s \quad (6)$$

From the sarcomere length the relative force (F_{rel}) can be derived (figure 2). The PCSA multiplied with $37 * 10^4 \text{ Nm}^{-2}$ (Weijs & Hillen, 1985) gives the maximum force possible. The real maximal force (F_{max}) and the maximal moment (M_{max}) can be calculated.

$$F_{max} = F_{rel} * PCSA * 37 \quad (7)$$

$$M_{max} = F_{max} * ma \quad (8)$$

Chapter 3 RESULTS

3.1 Cadaver measurements

Eight elbow muscles are dissected. Most of them are divided in different parts. Table 1 shows the number of muscle parts in which each elbow muscle is divided and the origin and insertion places of all muscles. The biceps caput longum is modelled as two functionally different muscles. The first part crosses the shoulder and its insertion is at the sulcus. This part has no effect on the elbow movement. The second part leads from the sulcus to the measured insertion place at the radius. This part is a flexor and a supinator. This division is made because the biceps caput longum crosses two joints and effects the movement of both joints.

The origin and insertions of the muscles are shown in table C1 (appendix C). The muscle length, fibre length, sarcomere length and mass of all muscles are measured. From these measurements, the other parameters are calculated. These parameters are given in table C2 and C3 (appendix C). The model also calculates muscle length in the anatomic state. In table C2 both measured and calculated lengths are given. There are some difference between those lengths.

Some muscles curve around one of the bones. Therefore the bone contours are measured. Through these data, cylinders are estimate (appendix C, table C4). With help of screw axes, the joint axes are calculated (appendix C, table C4).

3.2 Flexion extension movement

The model has calculated the length and moment arm of each muscle for 13 flexion angles with the forearm supinated. The change in length and moment arm for each muscle during flexion is shown in appendix D (figure D1 and D2).

From the muscle length, the fibre and sarcomere length of each muscle part are calculated for all flexion angles. Figure 6 shows the force/length relation of sarcomeres for the brachioradialis. The sarcomere length is plotted along the X-axis, the relative force along the Y-axis. Because the brachioradialis is divided in three parts, three lines are drawn. Two of the lines are transposed along the Y-axis.

Table 1

The elbow muscles.

The abbreviations (abbr.), the number (nr) of parts in which each muscle is divided and the place of origin and insertion of each elbow muscle.

Muscle	Abbr	Nr	Origin	Insertion
Biceps caput Breve	BIC br	2	Scapula	Radius
Triceps caput Longum	TR lg	4	Scapula	Ulna
Biceps caput Longum	BIC lg	1	Humerus	Radius
Triceps caput Mediale	TR md	5	Humerus	Ulna
Brachialis	BRACH	7	Humerus	Ulna
Brachioradialis	BRD	3	Humerus	Radius
Pronator Teres part Humerus	PT hum	1	Humerus	Radius
Pronator Teres part Ulna	PT uln	1	Ulna	Radius
Supinator	SUP	6	Ulna	Radius
Pronator Quadratus	PQ	3	Ulna	Radius
Triceps caput Laterale	TR lt	5	Humerus	Ulna
Anconeus	ANC	5	Humerus	Ulna

In this figure the sarcomere length of each muscle part is marked for five of the thirteen flexion angles with a circle and a number. It is shown that the sarcomere length declines during flexion. The relative force for each flexion angle can be derived from the figure. Figure D3 (appendix D) shows these figures for all muscles.

From the relative force, the maximum force and the maximal moment are calculated (figure 4 and 5 of appendix D). The maximal moments of the different muscle parts are combined for each muscle (figure 7). The flexors have positive moments and the extensors negative. The strongest flexors are the brachialis and the biceps. The brachioradialis and pronator teres are weak flexors. The triceps is the most important extensor. The anconeus has only a small flexion moment, although it has a large moment arm.

Brachioradialis

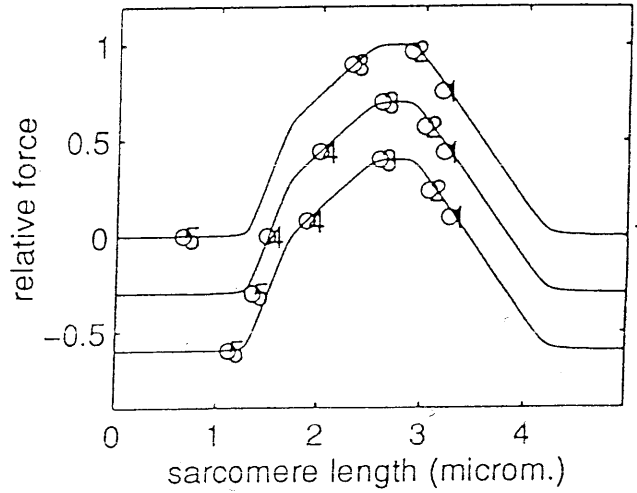


Figure 6

The Force length relation for the three parts of the brachioradialis. Two plots are transposed downwards. Five of the thirteen flexion angles are marked with a number in this figure.

- 1 : 0 degrees flexion
- 2 : 30 degrees flexion
- 3 : 60 degrees flexion
- 4 : 90 degrees flexion
- 5 : 120 degrees flexion

Moment of Flexion

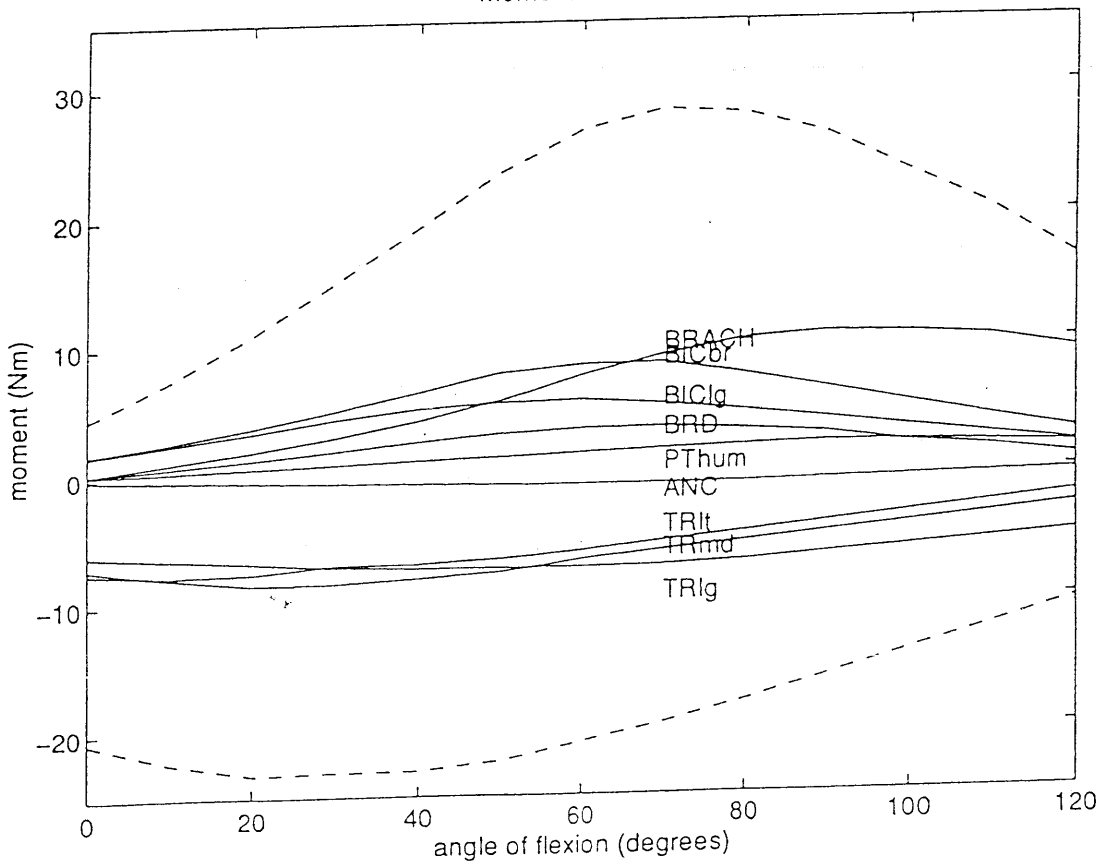


Figure 7 : Maximum moments by flexion.

The forearm is pronated. The positive moments are for flexion and the negative moments are for extension.

3.3 Pronation

For 5 different pronation angles with the elbow 90 degrees flexed, the model has calculated the muscle lengths and moment arms of all pronators and supinators. From these parameters the maximal force and moment are calculated like for flexion. In figure 1 to 5 of appendix E, the length, moment arm, sarcomere length, maximum force and maximum moment of these muscles are plotted against the pronation angle. The different maximum moments of all muscle parts are summed for each muscle and are shown in figure 8. Pronators have positive moments and the supinators have negative moments. The main pronators are the pronator teres and pronator quadratus. The supinator and biceps are used for supination. The brachioradialis has a pronation moment when the forearm is supinated and a supination moment when the elbow is pronated.

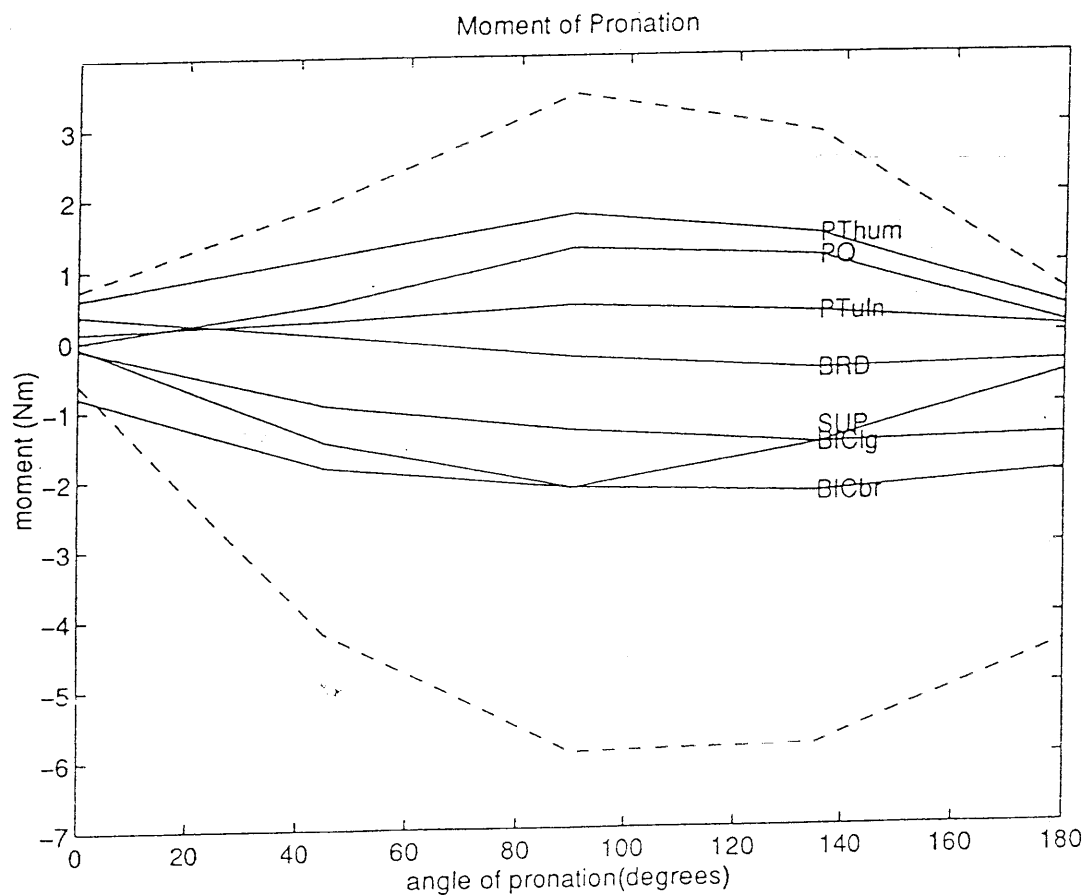


Figure 8 : Maximum moments by pronation.
The elbow is 90 degrees flexed. Pronators give positive moments and supinators give negative moments.

3.4 Influence of pronation and flexion on each other.

Three muscles have influence on both flexion and pronation. These are the biceps (caput longum and breve), the brachioradialis and the pronator teres (humerus part). In figure F1 to F4 (appendix F) the muscle length, moment arm, force and maximal moment are plotted against the flexion angle for 4 different pronation angles.

The maximum moment arm and the maximum force of the biceps are the same, but they are reached at a more flexed elbow in the case of a more pronated forearm. This results in a displaced maximum moment for a more pronated forearm.

The brachioradialis has for a more pronated elbow the same maximum moment arm at a slightly larger flexion angle. The same trend can be seen for the maximum force. The maximum moment is therefore reached at a larger flexion angle.

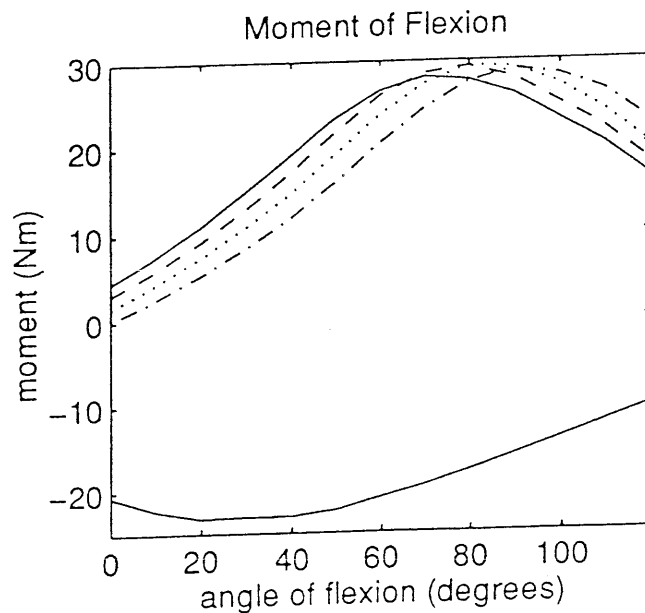
The moment arm of the pronator teres is larger for a more pronated forearm. The force reaches its maximum at a smaller flexion angle in the case of a more pronated forearm. These relationships combined, result in a maximum moment at a smaller flexion angle for a more pronated forearm. The highest maximum flexion moment is reached for a more neutral forearm.

The total maximum flexion moment of the elbow depends on the forearm position. Figure 9 shows a displaced maximum for a more pronated forearm. The maximum moment is slightly larger for a neutral forearm position.

The flexion moment does not change because of the pronation angle.

Figure 9
 Influence of pronation angle at the maximum flexion moment.
 Positive moments are flexion and negative moments are extension moments.

- : 0 degrees of pronation
 full supination
- : 45 degrees of pronation
- : 90 degrees of pronation
- .-.- : 135 degrees of pronation
 full pronation



Appendix G shows the influence of flexion on the change in length, moment arms, maximum force and maximum moments of the biarticular muscles during pronation. This parameters are calculated for an extended and a 90 degrees flexed elbow.

At extension the supination moment arm of the biceps is almost nil. The moment is therefore also almost zero. At 90 degree flexion, the biceps has a supination moment arm. The maximum force the biceps can deliver is also larger in case of a flexed elbow. The biceps has therefore a larger supination moment for a 90 degrees flexed elbow.

The brachioradialis has also an almost zero moment arm for an extended elbow. The moment arm changes for a 90 degrees flexed elbow from a pronation to a supination moment arm. The maximum force is almost constant for both flexion angles, but is larger in case of an extended elbow. The maximum moment changes also from pronation to supination moment when the elbow is 90 degrees flexed. The maximum moment is rather small, because the maximum force is rather small.

The pronator teres has a larger moment arm and a larger maximum force at a smaller pronation angle for a 90 degrees flexed elbow. Therefore the maximum pronation moment is larger and at a smaller pronation angle for the 90 degrees flexed elbow.

The flexion angle has a small influence on the maximal pronation moment and a large influence on the maximal supination angle (figure 10). A 90 degrees flexed elbow results in a larger maximal pronation and supination moment.

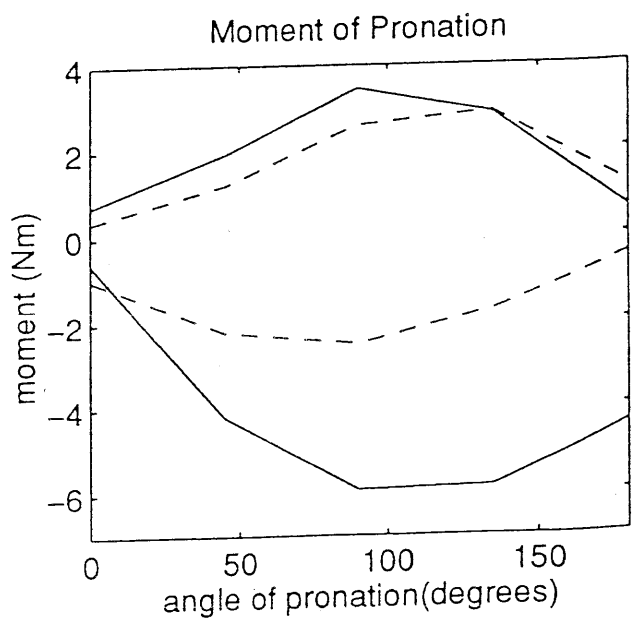


Figure 10
 Maximal pronation moment for two different flexion angles.
 Positive moments are pronation and negative moments are supination moments.
 — : 0 degrees flexed elbow full extended
 ---- : 90 degrees flexed elbow

CHAPTER 4 DISCUSSION

A complete parameter set of elbow muscles has been measured. A complete parameter set of shoulder muscles has already been measured at the same cadaver (Klein Breteler, 1996). These two datasets are combined and result in an unique shoulder-elbow muscle model.

4.1 Moment arms

There is a large deviation between measured moment arms of specimen. Murray (1995) has reviewed the flexion moment arms of different studies known from literature. She compared the biceps, the brachioradialis, the brachialis, the pronator teres and the triceps. Figure 11 shows these comparisons. The moment arms of the divided muscles of our study are placed in the same figure for comparison. The moment arms of the flexors are in the same range as the other moment arms measured. The triceps has a rather small moment arm compared to the moment arms of the other models. The estimation of the radius of the cylinder around which the triceps curves may be too small.

The moment arm of the anconeus has the same course as calculated by An et al (1981) and is in the same range as calculated by Amis et al (1979).

Just a few studies involved in pronation moment arms are done. The pronation moment arms used by Kleweno (1987) are much smaller than those calculated in this study. Kleweno estimated the attachment sites of the muscles. He modelled the muscles as straight lines, unless the smallest acceptable moment arm was reached. When the smallest acceptable moment arm was reached, the muscles curved around a spherical shell centred around the instant centre of the elbow joint. His data are estimations and not measurements like our data.

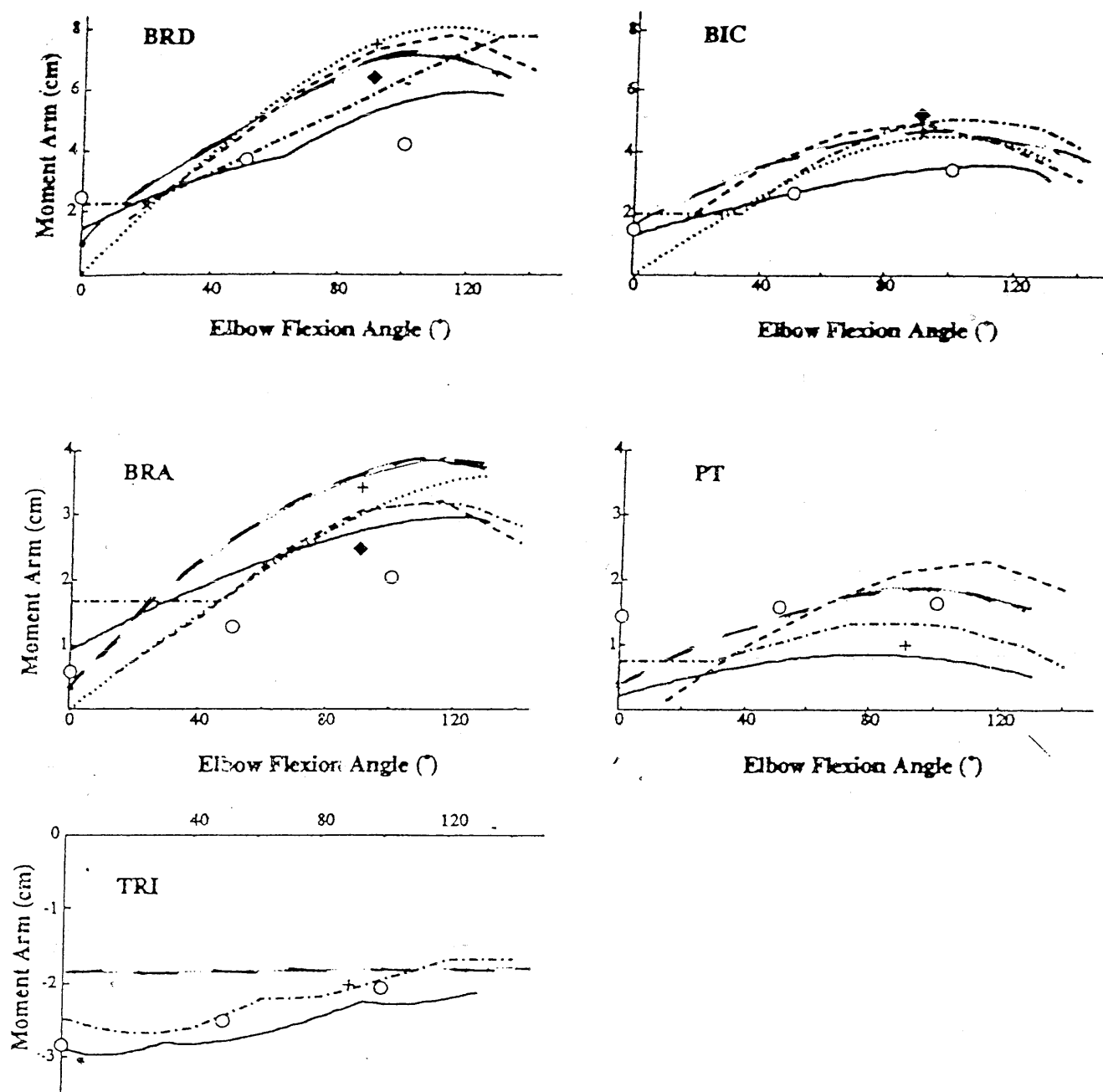


Figure 11
 Comparison of moment arms from different studies (Murray et al, 1995)

- Murray et al. (1995)
- .- Amis et al. (1979)
- Winter & Kleweno (1993)
- van Zuylen et al (1988)
- o An et al (1981)
- + An et al (1984)
- ◆ Crowninshield & Brand (1981)
- - Current study

4.2 Flexion forces and moments

Several investigators have measured the maximal flexion moment of the elbow in living persons. Most of the test persons are students or soldiers. There is a large variation between the results. The peak moment for males is found between 50 and 90 degrees flexion (Kleweno, 1987; Kullig et al, 1984; Knapik et al, 1983). The mean maximum measured peak moment is 69 ± 7 Nm (range between 50 and 100 Nm) for both the supinated and the pronated forearm. Females have a mean maximum moment of 46 ± 10.8 Nm at an angle between 50-100 degrees flexion. The maximal flexion moment for a neutral forearm position is about 25 percent higher, than when the forearm is pronated or supinated (Chaffin & Anderson, 1984; Jorgenson & Bankov, 1971; Singh & Karpovich, 1968). Other studies showed a larger flexion moment for a supinated forearm (Winter & Kleweno, 1993). The difference in maximum moments can be explained as a result of the biarticular muscles: the biceps, the brachioradialis and the pronator teres.

The maximum moment in this model is 29 Nm for flexion and 23 Nm extension. The maximum moment is reached at a flexion angle of 70 respectively 20 degrees. The maximum flexion moment of this study is at the same angle, but is much lower than seen at the measurements. There is only a small influence of forearm position at the maximal flexion moment.

Most model studies show a small maximum flexion moment compared to the measured moments. Most measurements are done at young healthy adults. The cadaver measured for this study is from an elderly man. The age and condition of people effect the muscle strength. This can be contributed to the discrepancy between models and measurements. The preparation of the cadaver may also influence the PCSA. The muscles may have shrunk due to the embalming.

An et al (1989) calculated 50 Nm as maximum flexion moment and Kleweno (1985) 62 Nm. The model of An et al (1989) is based on only three muscles: the biceps, the brachialis and the brachioradialis. Kleweno (1987) uses the same muscles as our model, but also the flexor carpi radialis longum and breve in his model. In table 2 the relative contributions of the different muscles to the maximum flexion moment are compared for this study and the studies of An et al (1989) and Kleweno (1985). The relative moments of An et al (1989) and our study are comparable. Kleweno estimates a rather high moment contribution for the brachioradialis and a low one for the brachialis.

Table 2

The relative moments of three studies (An et al, 1989; Kleweno, 1987). The maximum forces of all muscles are combined (row 2: total). The relative contribution of each muscles to the maximum moment is calculated. The second column of each study gives the flexion angle (degrees) belonging by the maximum moment. Kleweno uses different rest angles for all muscles. The averaged maximum moments of his calculations are taken.

	Kleweno (1987)		An et al (1987)		Our study	
	moment	angle	moment	angle	moment	angle
Total (Nm)	62	70-115	50	85	29	80
BIC	0.33	60-100	0.42	90	0.42	70
BRACH	0.24	60-120	0.40	85	0.42	90
BRD	0.18	60-120	0.18	90	0.11	80
PT	0.07	60 -95			0.05	120
ECRL	0.18	50-110				

The maximum force is calculated as the PCSA * P. P is a constant value for the maximum muscle stress. The value of P lays between 30 and 40*10⁴Nm⁻². In this study 37*10⁴Nm⁻² is used for P (Weijs & Hillen, 1985). Kleweno (1985) used 60*10⁴Nm⁻² for P. He did not explain his reasons. An et al (1987) used 100*10⁴Nm⁻² for P. They expected 50 Nm as maximum flexion moment (MacGarvey et al, 1984) and calculated P so that the maximum flexion moment was 50 Nm.

When the value P is set to 37*10⁴Nm⁻² for al three studies, the maximum flexion moments become 38.2, 18.5 and 29 Nm for Kleweno (1987), An et al (1989) and our study respectively.

The extensor carpi radialis longus and a few other muscles are not included in this model, because the model has not enough space. The muscle parameters are measured for the extensor carpi radialis. The PCSA is 4.137cm² and the moment arm is about 2 cm. The muscle would give a moment of about 3 Nm in this model. When the extensor carpi radialis longus is taken into account, the total moment would increase to 32 Nm.

The most important flexor is as expected the triceps. The anconeus has just a very small moment. The function of the anconeus is not known (Basmajian et al, 1972). It is most likely that the anconeus is a joint stabilizer. This study gives no evidence for that hypothesis.

4.3 Pronation and supination moments

Little research has been done concerning the moments during pronation and supination (Darcus, 1951; Kleweno, 1987). The maximum pronation and supination moment in both studies increases during pronation. In this research, there is a maximum pronation and supination moment for a pronation angle of 80 respectively 120 degrees. The pronator quadratus, the pronator teres and the supinator curve around both the radius and the ulna. In the model, just one of the bones is taken into account. It may be that two cylinders should be used for a more accurate description of these muscles.

The maximum pronation moment of this study is about 3.5 Nm and the maximum supination moment is about 6 Nm. The maximum measured moments by Darcus (1951) and Kleweno (1987) are 10 and 11 Nm for pronation and 9 and 11 Nm for supination respectively. Even as for flexion the measured moments are higher than the by the model calculated moments .

4.4 Recommendations

There is evidence that the extensor carpi radialis longus and brevis are small flexors. A better elbow model would be developed, when these muscles are also implanted in the model.

The pronator teres, the pronator quadratus and the supinator are curved around two bones. A better description of these muscles would be when both bones are implanted in the model.

The biceps caput longum should be modelled as one part. Therefore two spherical shells are necessary. Then, the influence of biarticular shoulder/elbow muscles can be studied. For a total arm model the muscles crossing the carpal joint have to be modelled.

REFERENCES

- Amis, A.A., Downson, D. and Wright, V (1979) Muscle strengths and musculoskeletal geometry of the upper limb. *Engng Med.* **8**, 41-48.
- An, K.N., Hui, F.C., Morrey, B.F., Linscheid, R.L. and Chao, E.Y. (1981) Muscles across the elbow joint: A biomechanical Analysis. *J.Biomechanics* **14**, 659-669.
- An, K.N., Kwak, B.M. and Chao, E.Y. (1984) Determination of muscle and joint forces: a new technique to solve the indeterminate problem. *J.Biomech. Engng* **106**, 364-367.
- An, K.N., Kaufman, K.R. and Chao, E.Y. (1989) Physiological considerations of muscle force through the elbow joint. *J.Biomechanics* **22**, 1249-1256.
- Bagni, M.A., Cecchi, G., Colomo, F. and Tesi, C. (1986) The sarcomere length-tension relation in short length-clamped segments of frog single muscle fibres. *J of Physiology* **377**: 31P.
- Basmajian, J.V. and Griffin, W.R. jr. (1972) Function of Anconeus Muscle, An electromyographic Study. *J. Bone and Joint Surg.* **54A(8)**, 1712-1714.
- Chauffin, D.B. and Anderson, .B.H. (1984) Occupational Biomechanics. *Hafner*, New York.
- Crowninshield, R.D. and Brand, R.A. (1981) A physiologically based criterion of muscle force predication in locomotion. *J. Biomechanics* **14**, 793-801.
- Darcus, H.D. (1951) The maximum torques developed in pronation and supination of the right hand. *J. Anatomy* **85**, 55-67.
- Fick, R. (1929) Handbuch der Anatomie und Mechanik der Gelenke. *Gustav Fischer*, Jena.

- Huxley, A.F. and Niedergerke, R. (1954) Structural changes in muscle during contraction; interference microscopy of living muscle fibres. *Nature* **173**, 971-973.
- Huxley, H.E. (1957) The double array of filaments in cross-striated muscles. *J. of Biophysics and Biochemical Cytology* **3**, 631-648.
- Jonker, B. (1988) A finite element dynamical analysis of flexible spatial mechanism and manipulators. *Doctoral thesis*, Delft University of Technology, Delft, The Netherlands.
- Jorgenson, K. and Bankov, S. (1971) Maximum strength of elbow flexors with pronated and supinated forearm. *Med. and Sport 6: Biomechanics II*. 174-180, Baltimore, MD.
- Klein Breteler, M. (1996) Measuring muscle joint and geometry parameters for a shoulder model. *Thesis*. Faculty of Human Movement Science, Vrije Universiteit, Amsterdam.
- Kleweno, D.G. (1987) Physiological and theoretical analysis of isometric strength curves of the upper limb. *Doctoral Thesis*. Arizona state university, USA.
- Knapik, J.J., Wright, J.E., Mawdsley, R.H. and Braun, J. (1983) Isometric, isotonic and isokenetic torque variations in four muscle groups through a range of joint motions. *Phys. Ther.* **63(6)**, 938-947.
- Kullig, K., Andrew, J.G. and Hay, J.G. (1984) Human strength curves. *Exerc. Sport Sci. Rev.* **1986**, 417-566.
- Larson, R.F. (1969) Forearm positioning on maximal elbow flexor force. *Phys. Ther.* **49(7)**, 748-756.
- MacGarvey, S.R. Morrey, B.F., Askew, L.J. and An, K.N. (1984) Reliability of isometric strength testing: temporal factors and strength variation. *Clin.ortop. Rel. Res.* **185**, 301-305.

Murray, W.M., Delp, S.L. and Buchanan, T.S. (1995) Variations in muscle moment arms with elbow and forearm position. *J. Biomechanics* (28(5), 523-525.

Pronk, G.M. (1991) The shoulder girdle *Doctoral thesis* Delft Technical University, ISBN 90-370-0053-3.

Salter, N. and Darcus, H.D. (1957) The effect of the degree of elbow flexion on the maximal torques developed in pronation and supination of the right hand. *J. Anatomy* **86**, 197-202.

Singh, M and Karpovich, P.V. (1986) Strength of forearm flexors and extensors in men and women. *J. Biomechanics* **6**, 79-92.

Van der Helm, F.C.T. (1988) A dynamical model of the shoulder girdle. In *Abstracts: 6th Meeting of the European Society of Biomechanics*, abstract No. B26, Bristol, England.

Van der Helm (1994) Analysis of the kinematic and dynamic behaviour of the shoulder mechanism. *J. of Biomechanics* **27(5)**, 527-550.

Van der Helm (1994) A finite element musculoskeletal model of the shoulder model. *J. of Biomechanics* **27(5)**, 551-569.

Van der Helm, F.C.T. and Pronk, G.M. (1989) A finite element musculoskeletal model of the shoulder mechanism. *Proceedings of the 2nd International Symposium on Computer Simulation in Biomechanics*, Davis CA. 36-37.

Van der Helm, F.C.T., Veeger, H.E.J., Pronk, G.M., Van der Woude, L.H.V. and Rozendal, R.H. (1992) Geometry parameters for musculoskeletal modelling of the shoulder system. *J. Biomechanics* **25**, 129-144.

- Van Zuylen, E.J., van Velzen, A. and Denier van der Gon, J.J. (1988) A biomechanical model for flexion torques of human arm muscles as a function of elbow angle. *J. Biomechanics* **21**, 183-190.
- Walker, S.M. and Schrodt, G.R. (1974) I segmental lengths and thin filament periods in skeletal muscle fibres of the rhesus monkey and human. *Anatomical Record* **178**, 63-82.
- Weijts W.A. and Hillen B. (1985) Cross-sectional Areas and Estimated Intrinsic Strength of the Human Jaw muscles. *Acta Morphol. Neerl.-Scand.* **23**, 267-274.
- Werff, K. van der (1977) Kinematic and dynamic analysis of mechanism: A finite element approach. *Doctoral thesis*, Delft University of Technology, Delft, The Netherlands.
- Werff, K. van der and Jonker, B. (1983) Dynamics of flexible mechanism. in *4Proc. NATO Advanced Study Inst. on Computer Aided Analysis and Optimization of Mechanical System Dynamics*, Iowa City, 381-400.
- Winter, J. Stark, L. and Seif- Naraghi, A.H. (1988) An analysis of the sources of musculoskeletal system impedance. *J. Biomechanics* **21** 1011-1025.
- Winters, J.M. and Kleweno, D.G. (1993) Effect of initial upperlimb alignment on muscle contributions to isometric strength curves. *J. Biomechanics* **26** 143-153.
- Winters, J.M. and Stark, L. (1985) Analysis of fundamental human movement patterns through the use of in-depth antagonistic muscle models. *Ieee Transaction on biomedical engineering* **10**, 826-839.

APPENDIX A

REM Data-Shoulder-Project
 REM This file includes multinode elements and a moving thorax.
 REM
 REM febr.-juli, 1995 , Mary Klein Breteler
 REM Change of the axes 25-10-1996, Joanne Minekus
 REM Expanded with the elbow 10/96-6/97

REM global thorax orientation:
 HINGE 1 1 2 1 0 0
 HINGE 2 2 3 0 1 0
 HINGE 3 3 4 0 0 1
 FIX 1 2 FIX 1 3 FIX 1 4

REM sternoclavicular joint:
 HINGE 4 4 5 0 1 0
 HINGE 5 5 6 0 0 1
 HINGE 6 6 7 1 0 0
 RLSE 4 1 RLSE 5 1 RLSE 6 1

REM acromioclavicular joint:
 HINGE 7 7 8 0 1 0
 HINGE 8 8 9 0 0 1
 HINGE 9 9 10 1 0 0
 RLSE 7 1 RLSE 8 1 RLSE 9 1

REM glenohumeral joint:
 HINGE 10 4 11 1 0 0
 HINGE 11 11 12 0 1 0
 HINGE 12 12 13 0 0 1

REM humero-ulnar joint:
 HINGE 13 13 14 0.8958 0.0149 -0.4318
 HINGE 14 14 15 0 1 0
 HINGE 15 15 16 0 0 1

REM ulnar-radial joint:
 HINGE 16 16 17 -0.0259 0.9931 0.1141
 HINGE 17 17 18 0 0 1
 HINGE 18 18 19 0 1 0

REM radial-carpal joint:
 HINGE 19 19 20 1 0 0
 HINGE 20 20 21 0 1 0
 HINGE 21 21 22 0 0 1

REM thorax (elementnr,position node,orientation node)
 REM center of gravity is center of ellipsoid
 MNODEDEF 22 23 4
 X 23 0 -13.93 6.799

REM clavicle (elementnr,position node,orientation node)
 MNODEDEF 23 24 7
 X 24 8.435 1.224 5.025

APPENDIX D : FIGURES OF FLEXION

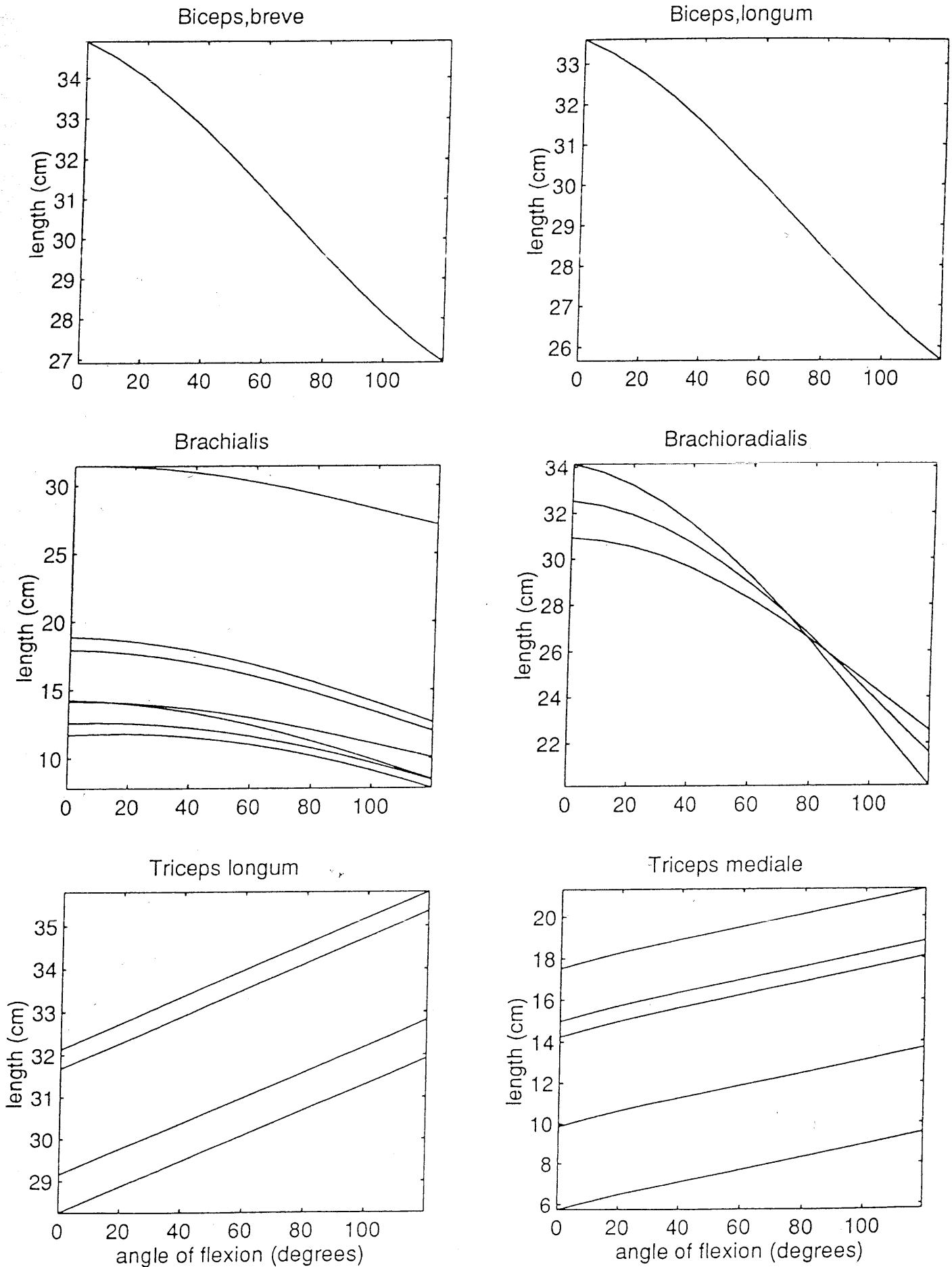


Figure D1 : Change in muscle length during flexion (1)
The forearm is supinated.

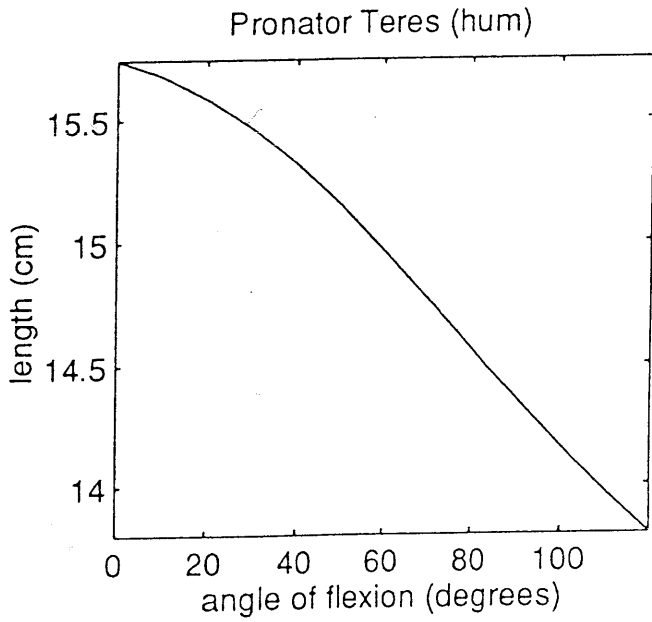
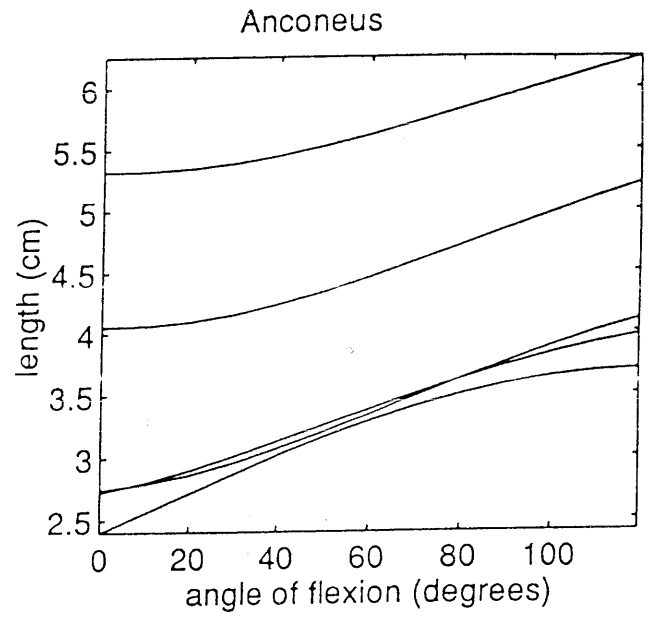
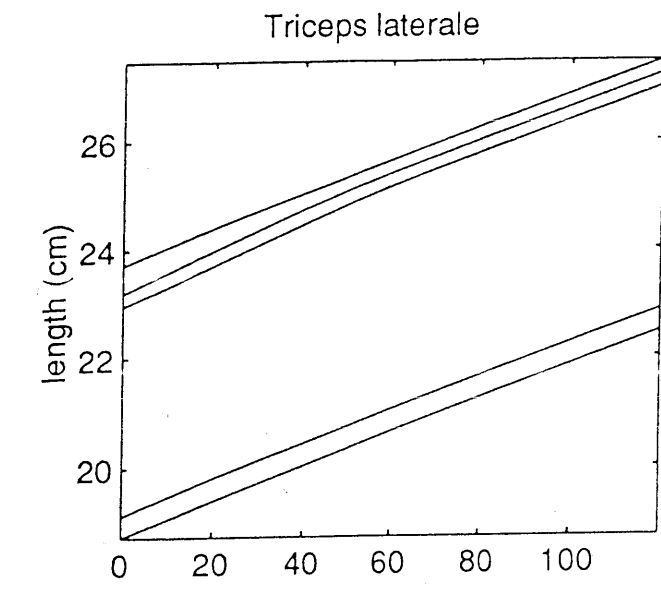


Figure D1 : Change in muscle length during flexion (2)
The forearm is supinated.

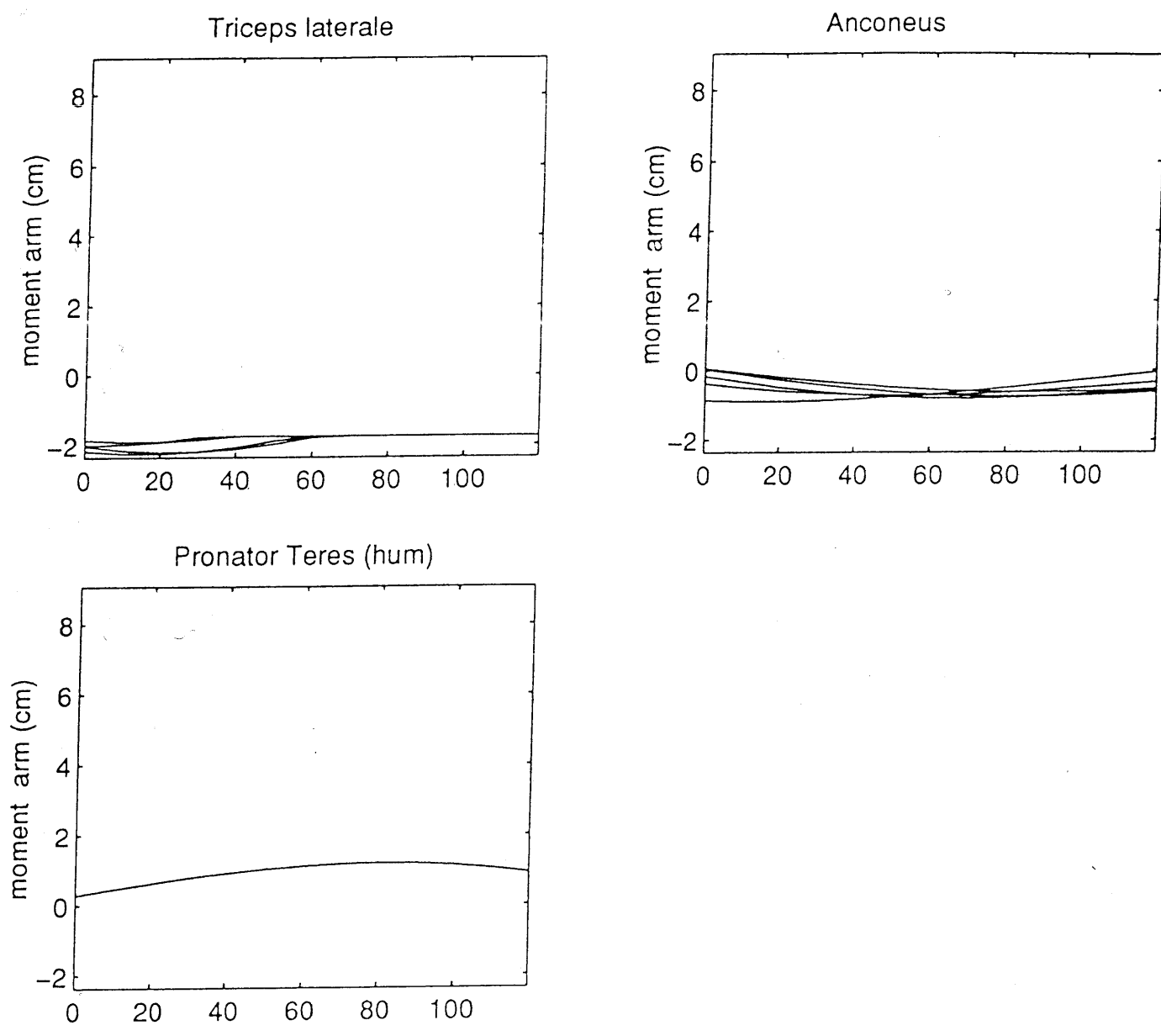
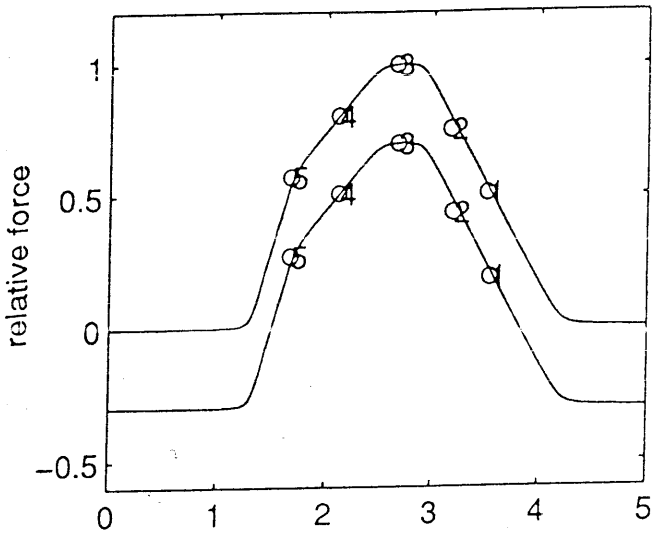
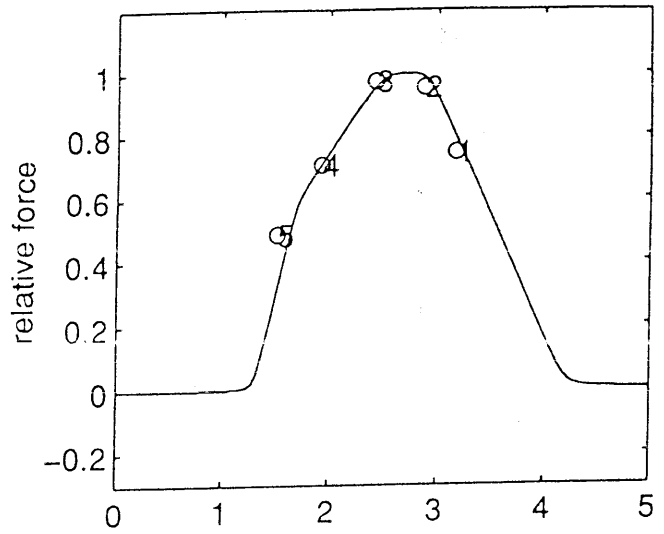


Figure D2 : Change in moment arm during flexion (2)
The forearm is supinated.

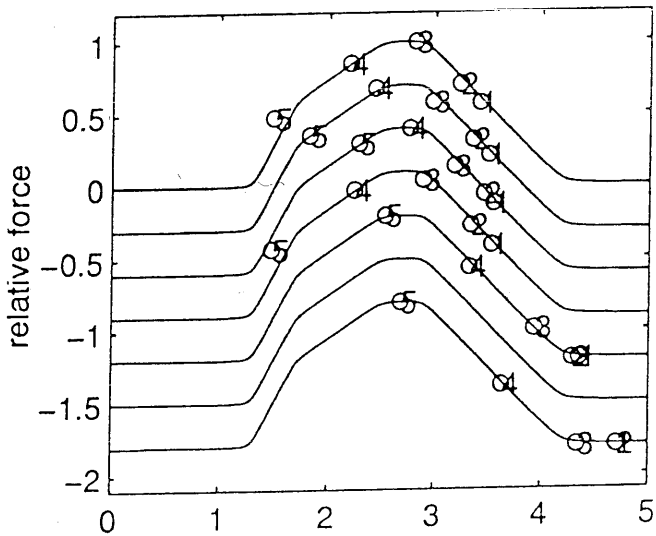
Biceps,breve



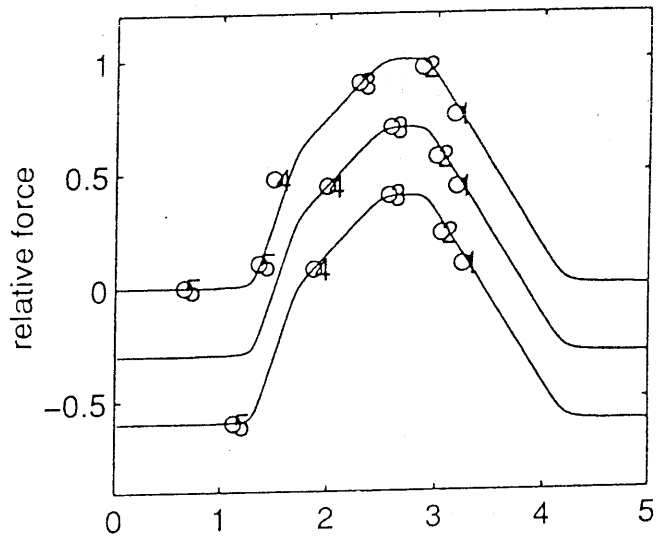
Biceps longum



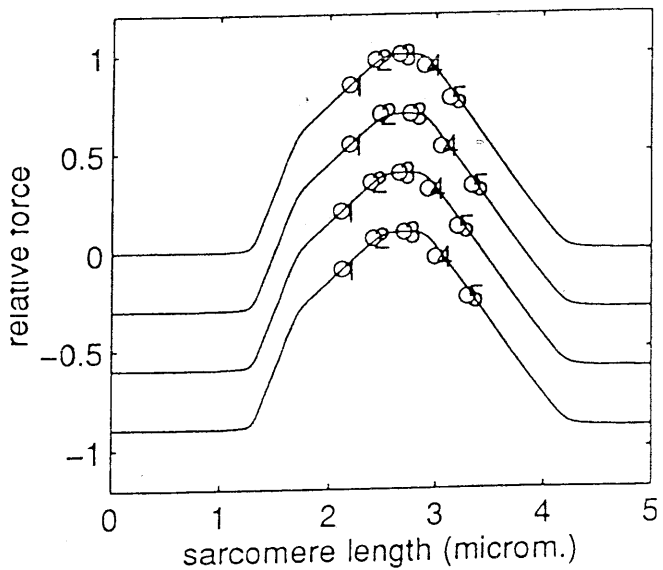
Brachialis



Brachioradialis



Triceps,longum



Triceps mediale

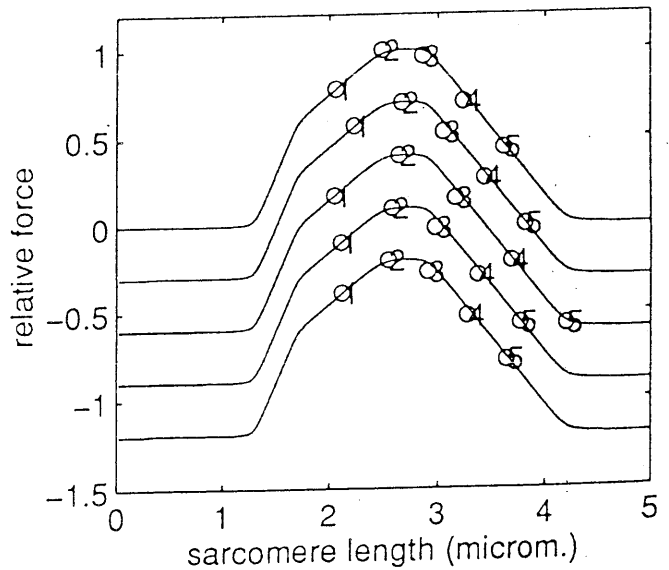


Figure D3 : Force length relation of sarcomeres for flexion(1)
The forearm is suninated.

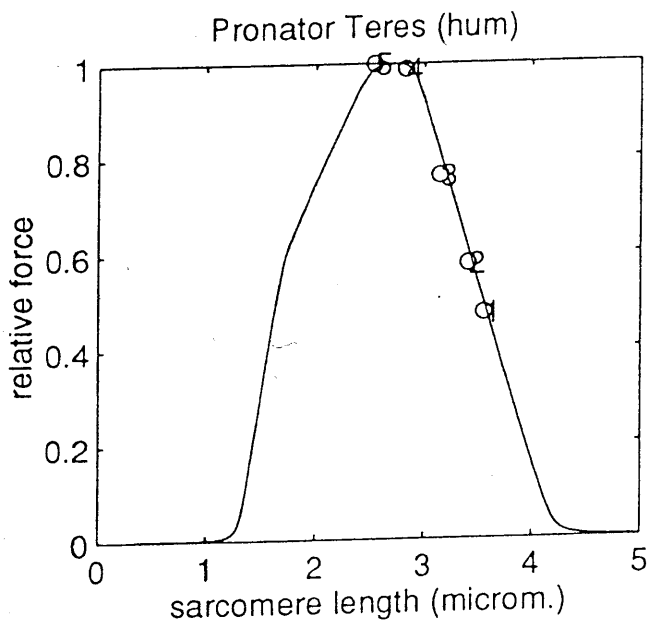
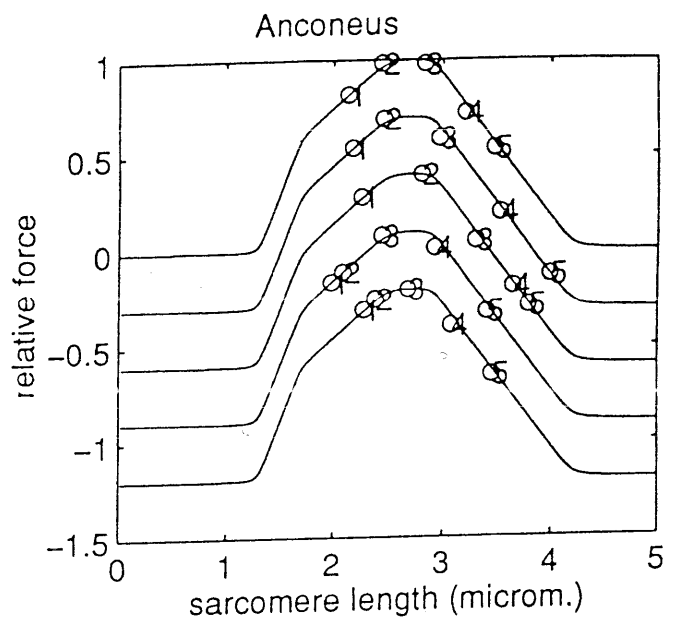
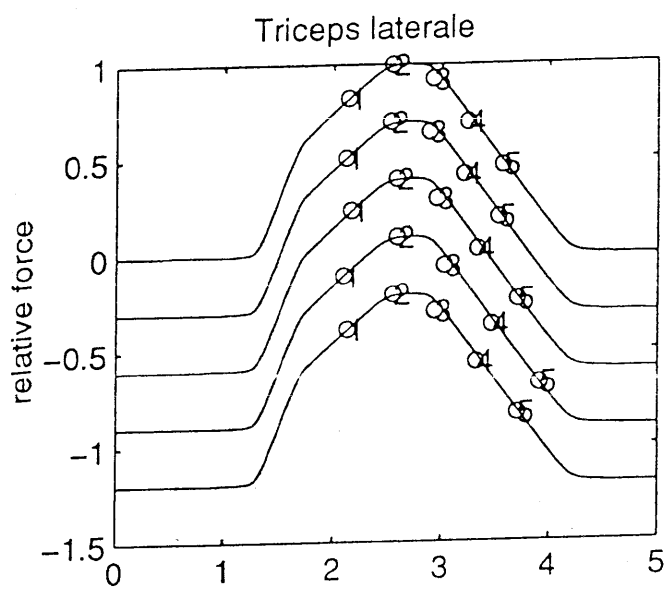


Figure D3 : Force length relation of sarcomeres for flexion(2)

The forearm is supinated.

- 1 : 0 degrees of flexion
- 2 : 30 degrees of flexion
- 3 : 60 degrees of flexion
- 4 : 90 degrees of flexion
- 5 : 120 degrees of flexion

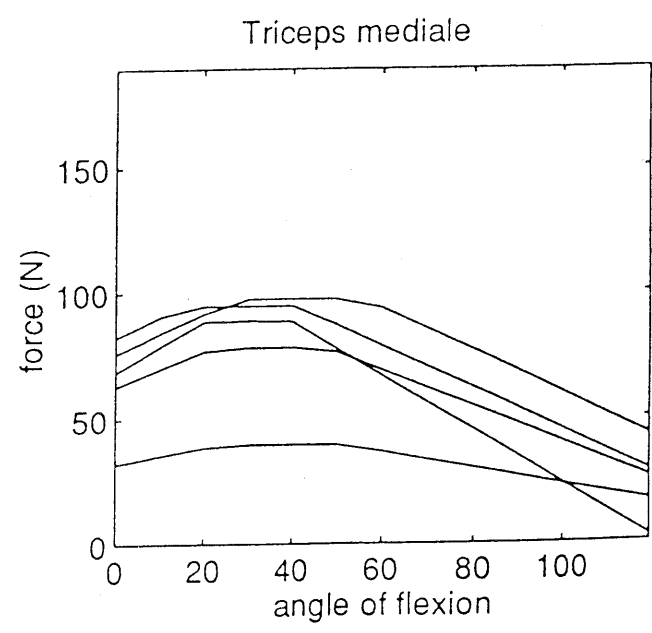
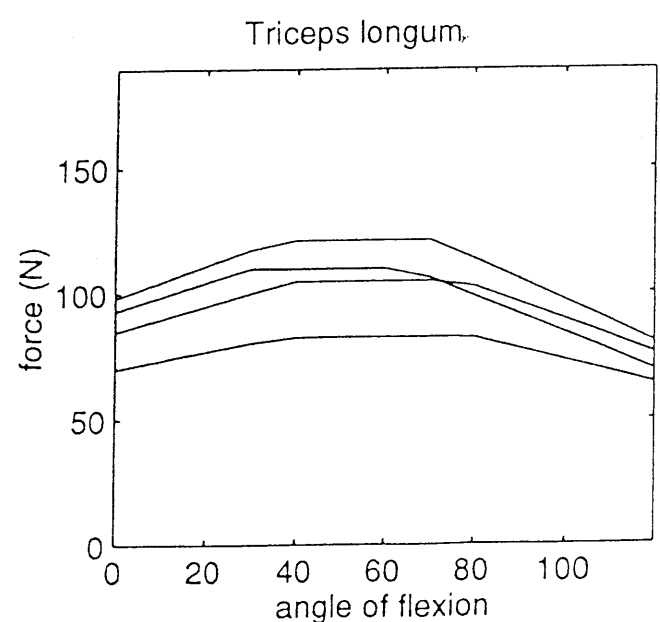
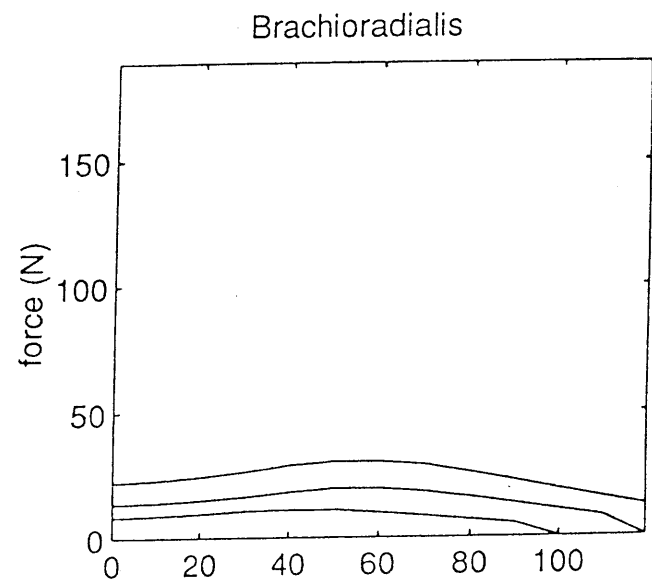
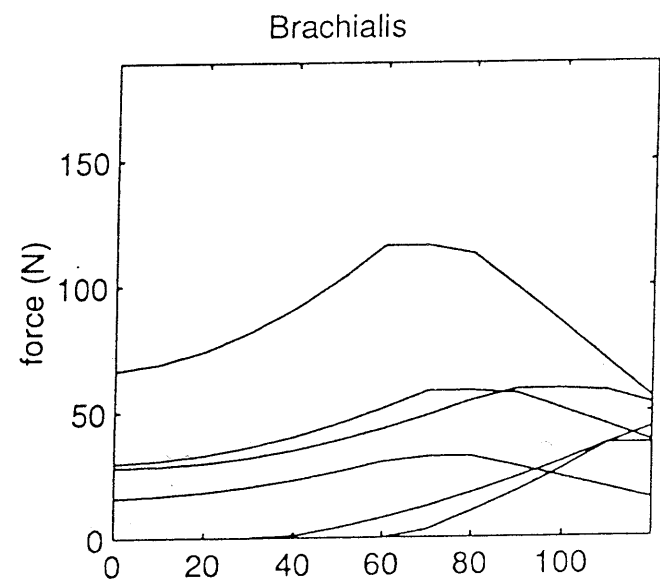
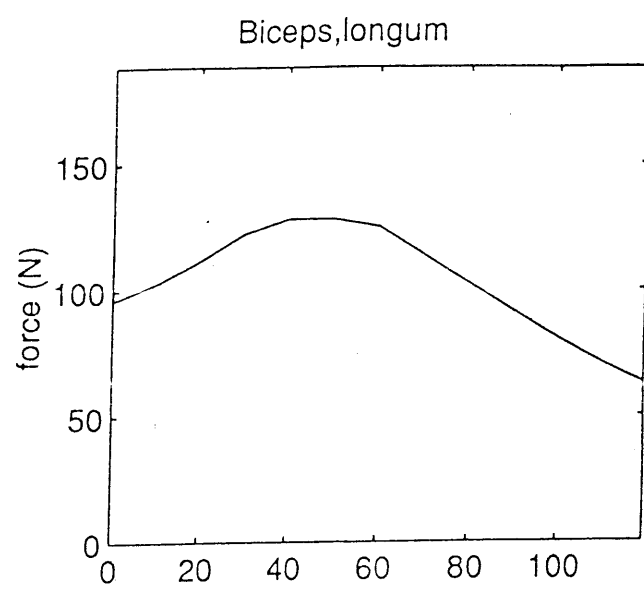
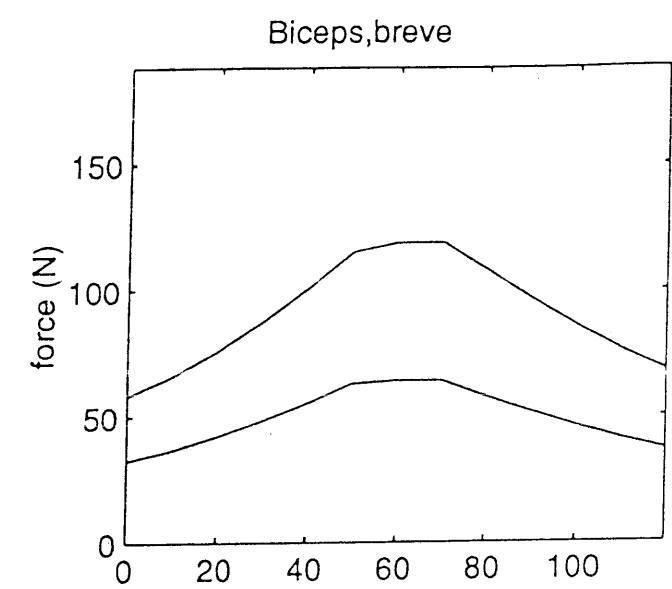


Figure D4 : Maximum force by flexion (1)
The forearm is supinated.

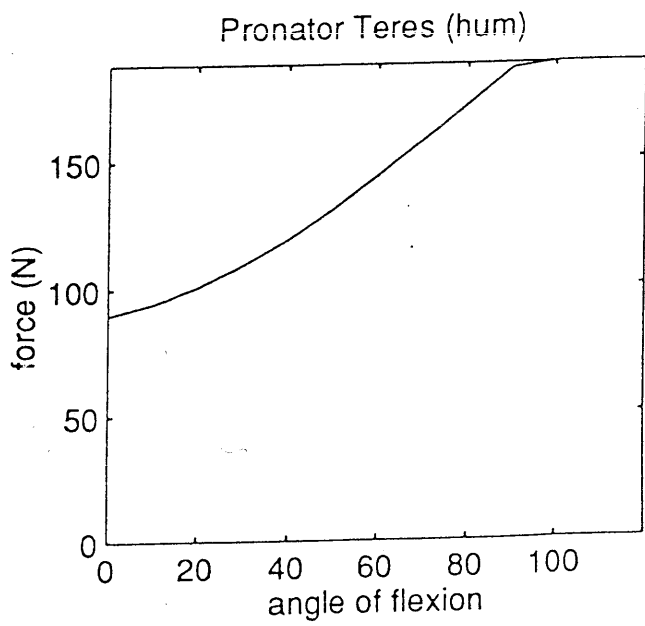
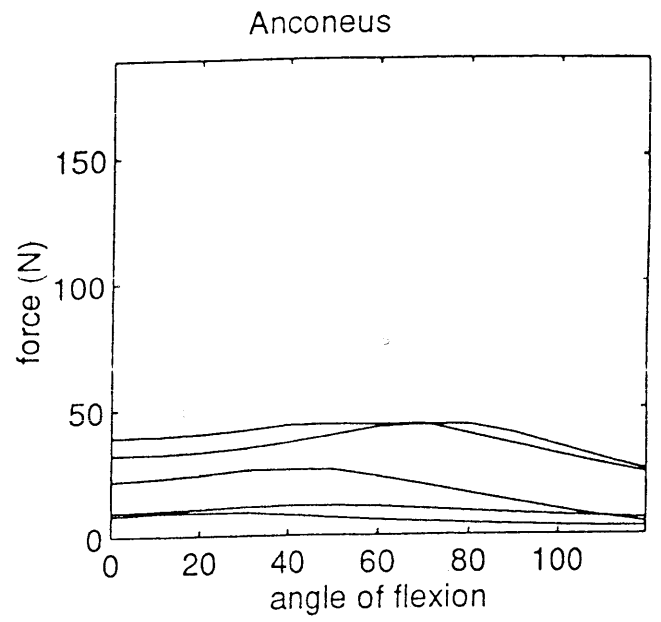
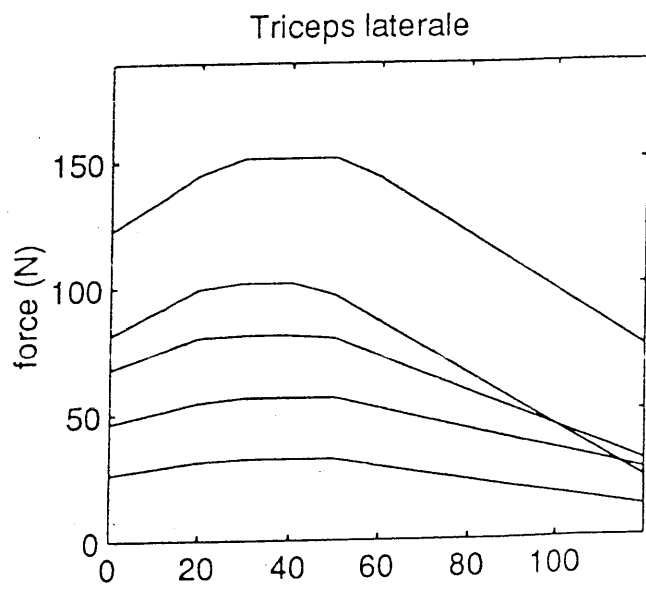
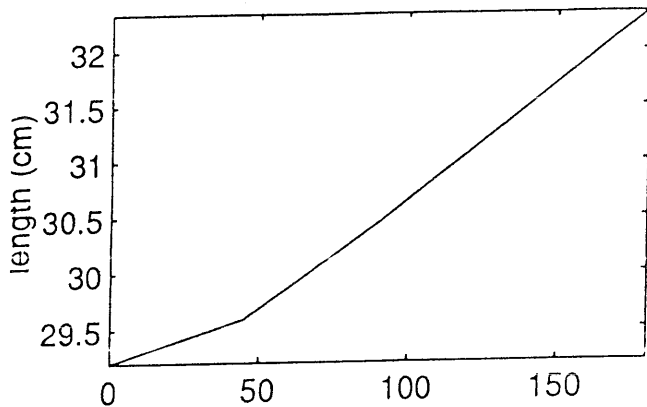


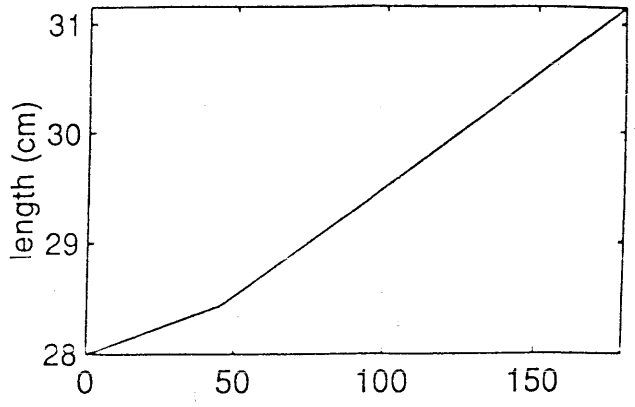
Figure D4 : Maximum force by flexion (2)
The forearm is supinated.

APPENDIX E : FIGURES OF PRONATION

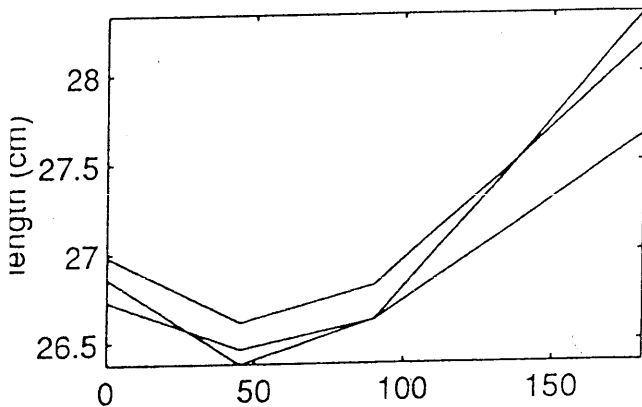
Biceps,breve



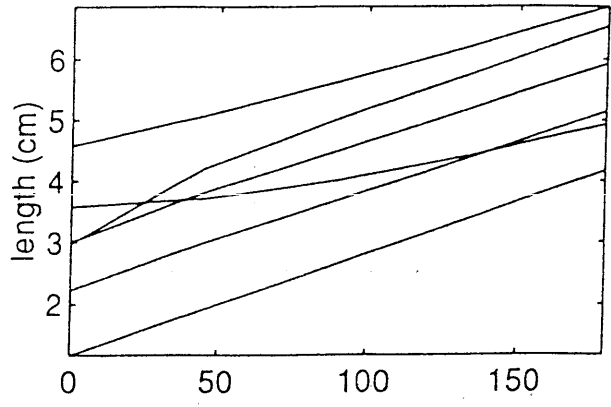
Biceps,longum



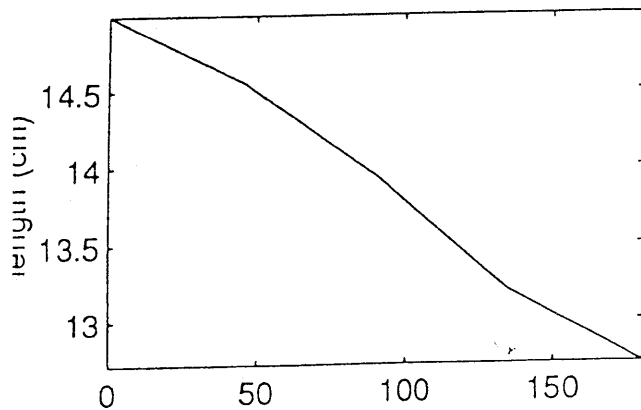
Brachioradialis



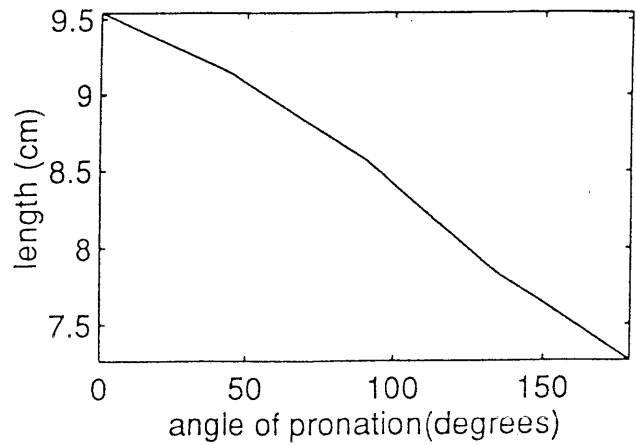
Supinator



Pronator Teres (hum)



Pronator Teres (ulna)



Pronator Quadratus

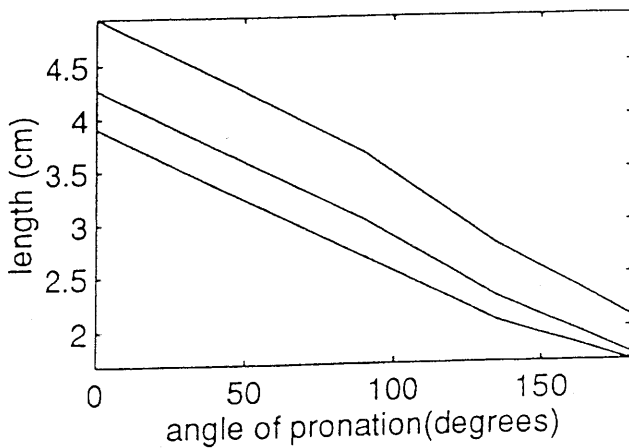


Figure E1 : Change in muscle length during pronation. The elbow is 90 degrees flexed.

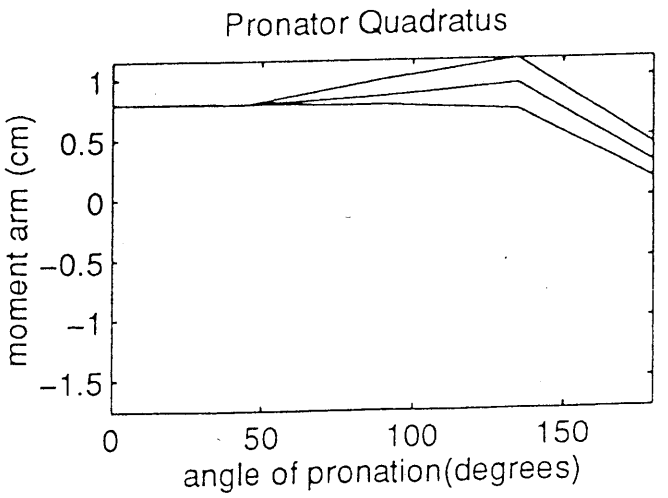
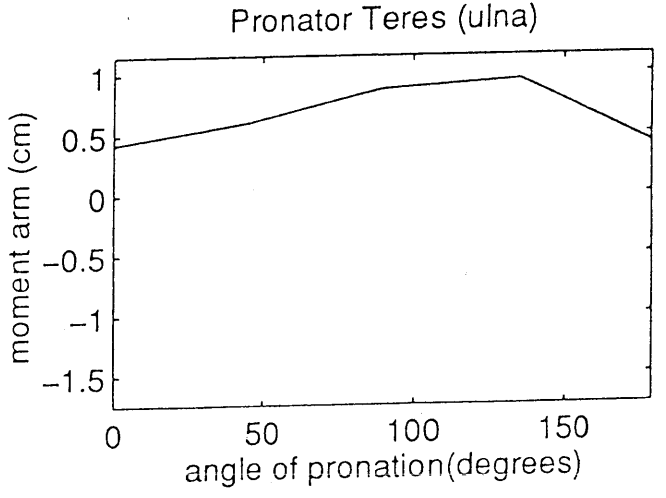
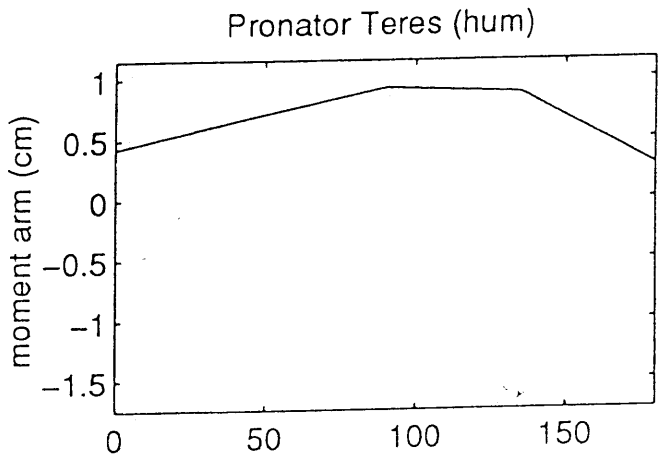
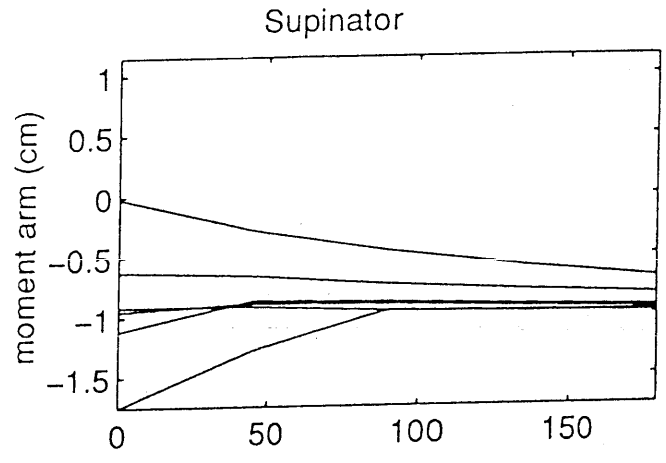
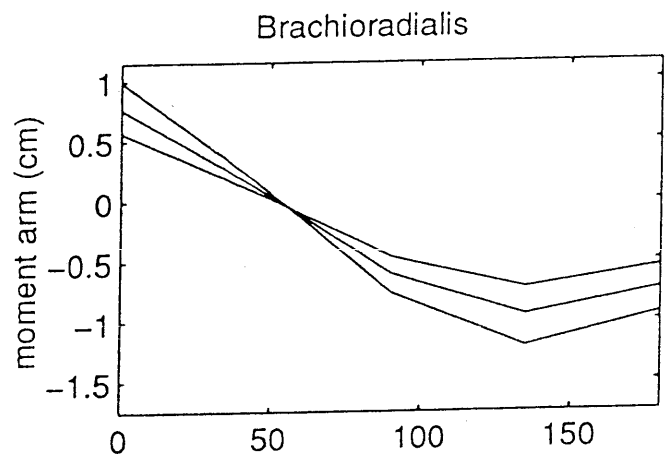
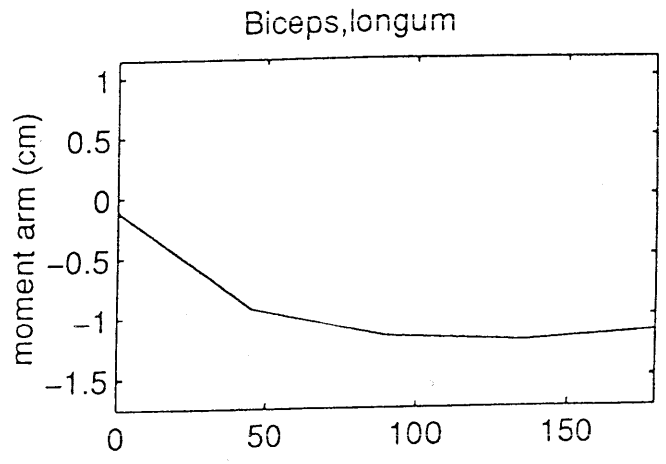
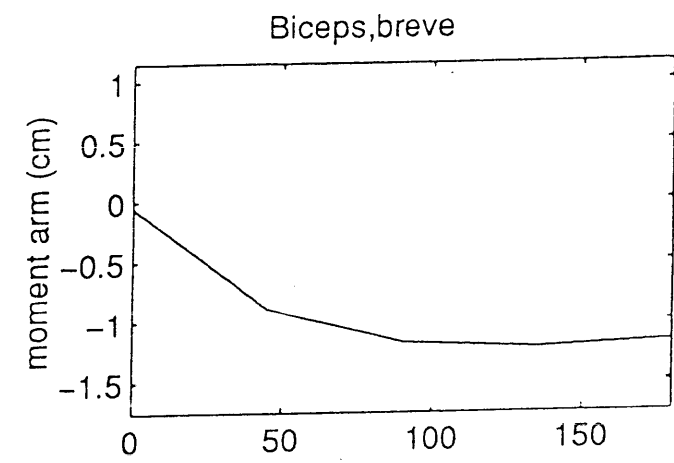


Figure E2 : Change in moment arm during pronation. The elbow is 90 degrees flexed.

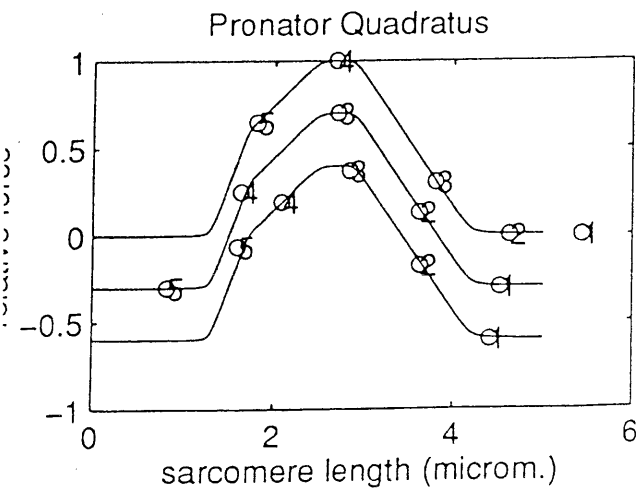
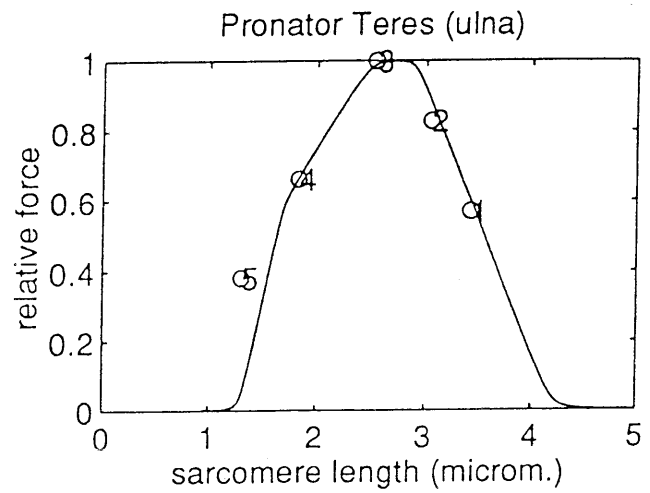
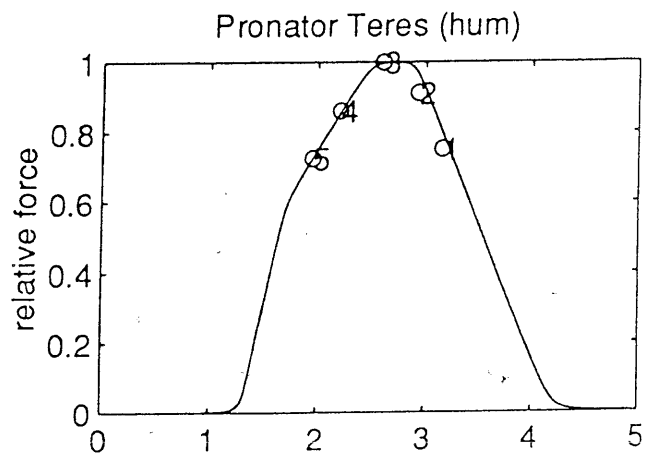
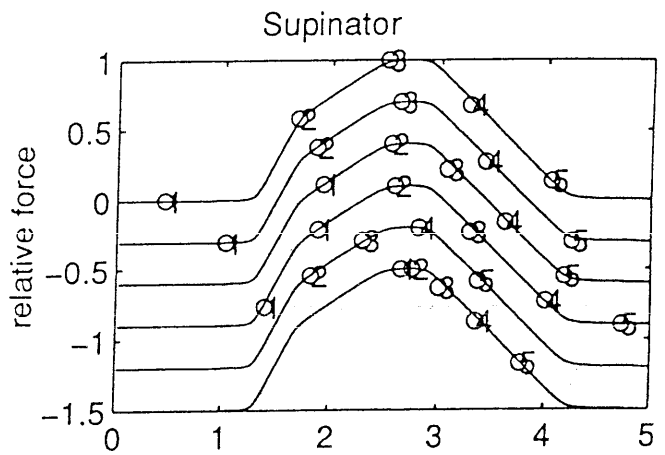
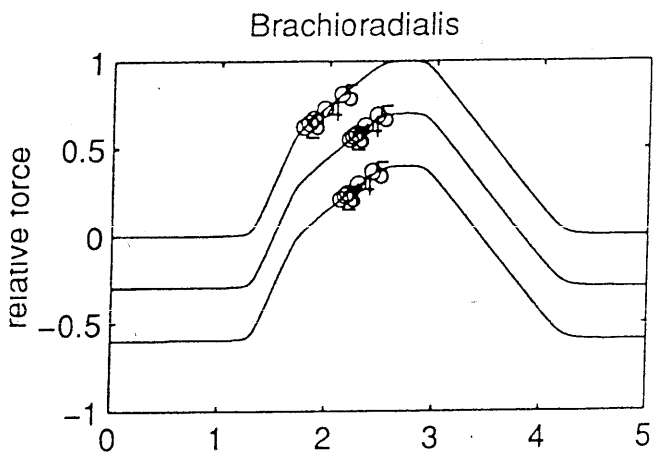
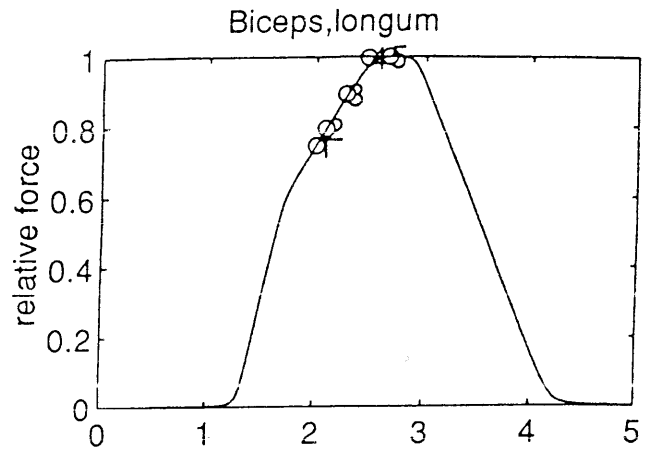
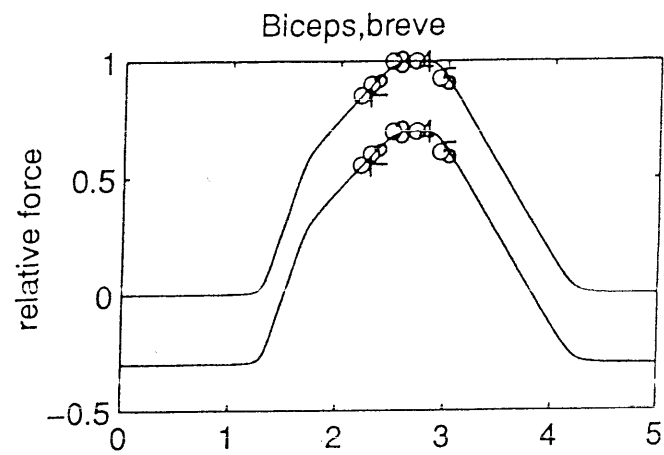


Figure E3 : Force length relation of sarcomeres for pronation.
 The elbow is 90 degrees flexed.

- 1 : 0 degrees of pronation
- 2 : 45 degrees of pronation
- 3 : 90 degrees of pronation
- 4 : 135 degrees of pronation
- 5 : 180 degrees of pronation

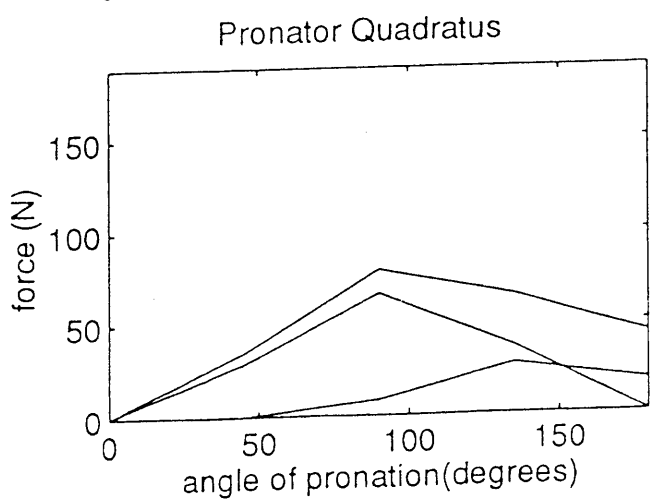
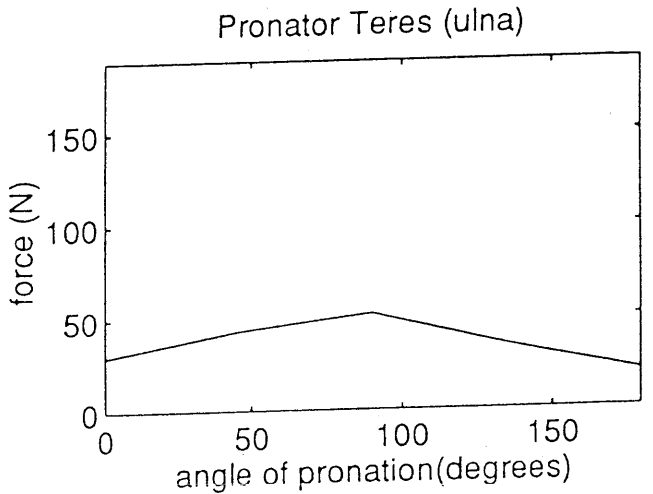
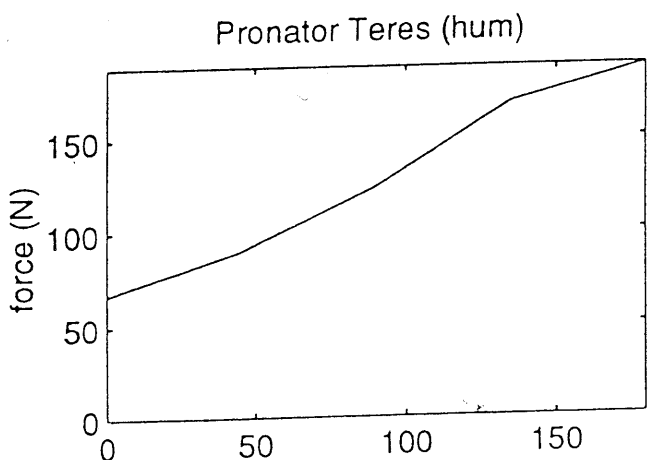
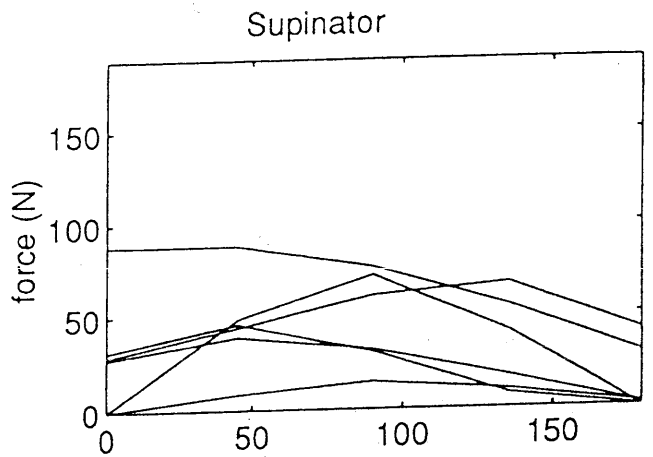
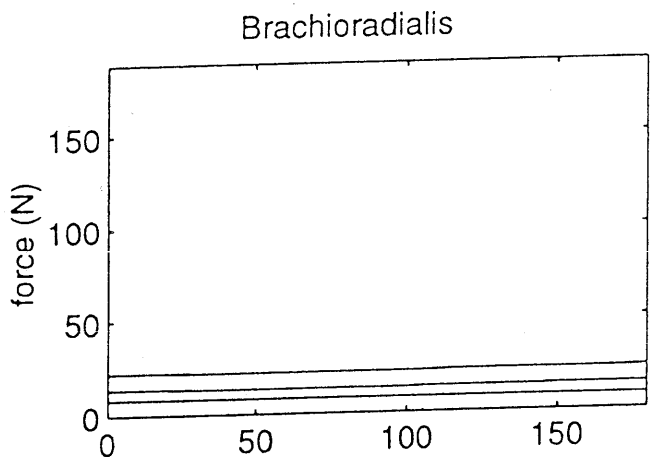
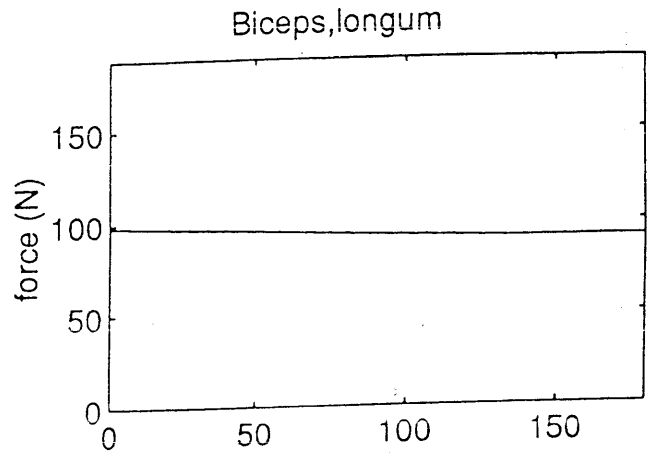
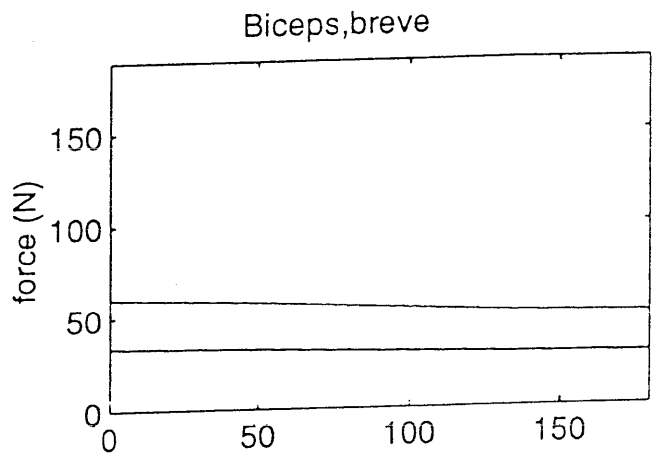
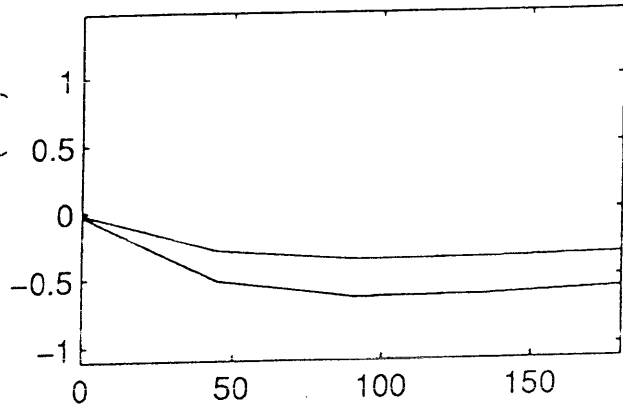
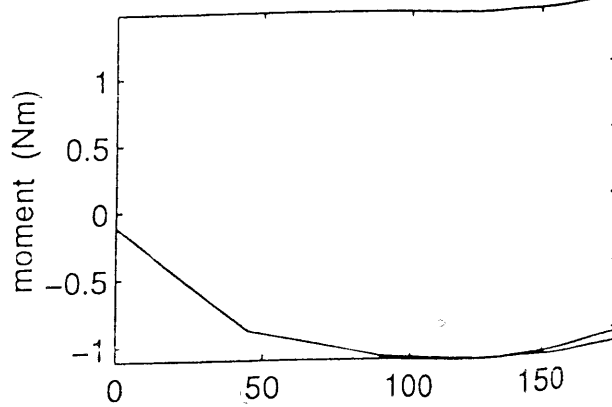


Figure E4 : Maximum force by pronation.
The elbow is 90 degrees flexed.

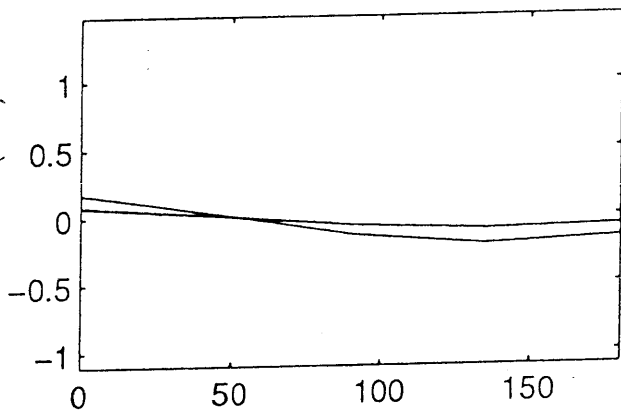
Biceps,breve



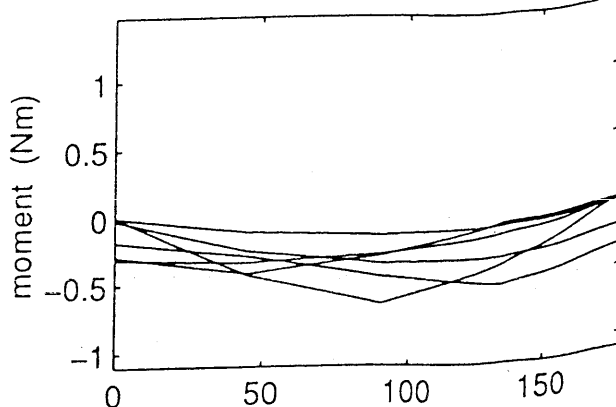
Biceps,longum



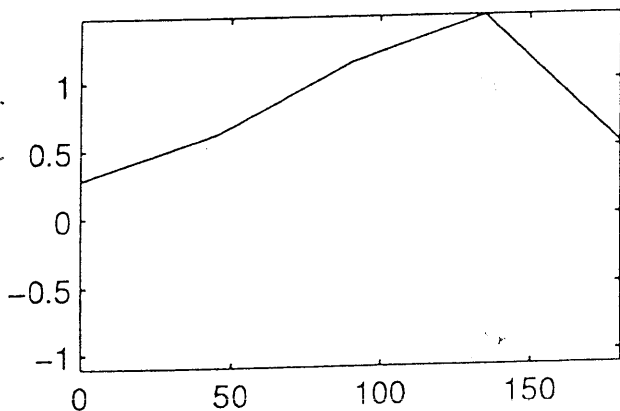
Brachioradialis



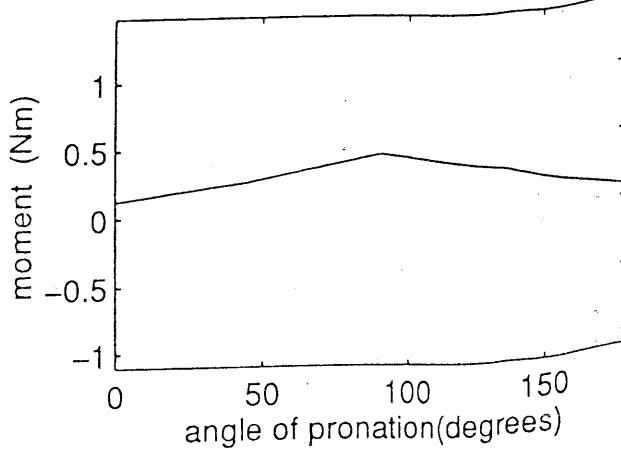
Supinator



Pronator Teres (hum)



Pronator Teres (ulna)



Pronator Quadratus

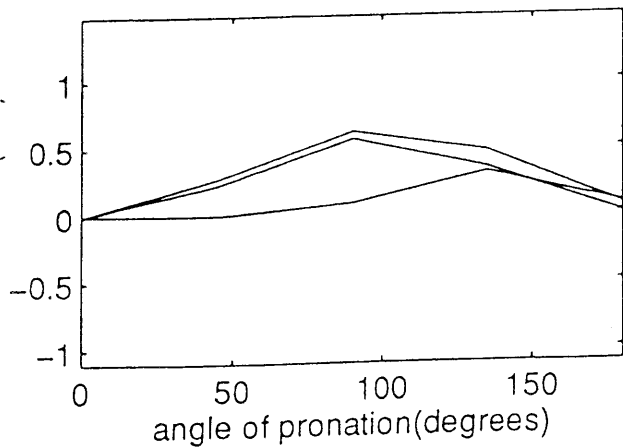


Figure E5 : Maximum moment by pronation
The elbow is 90 degrees flexed.

APPENDIX F : EFFECT OF PRONATION ON FLEXION

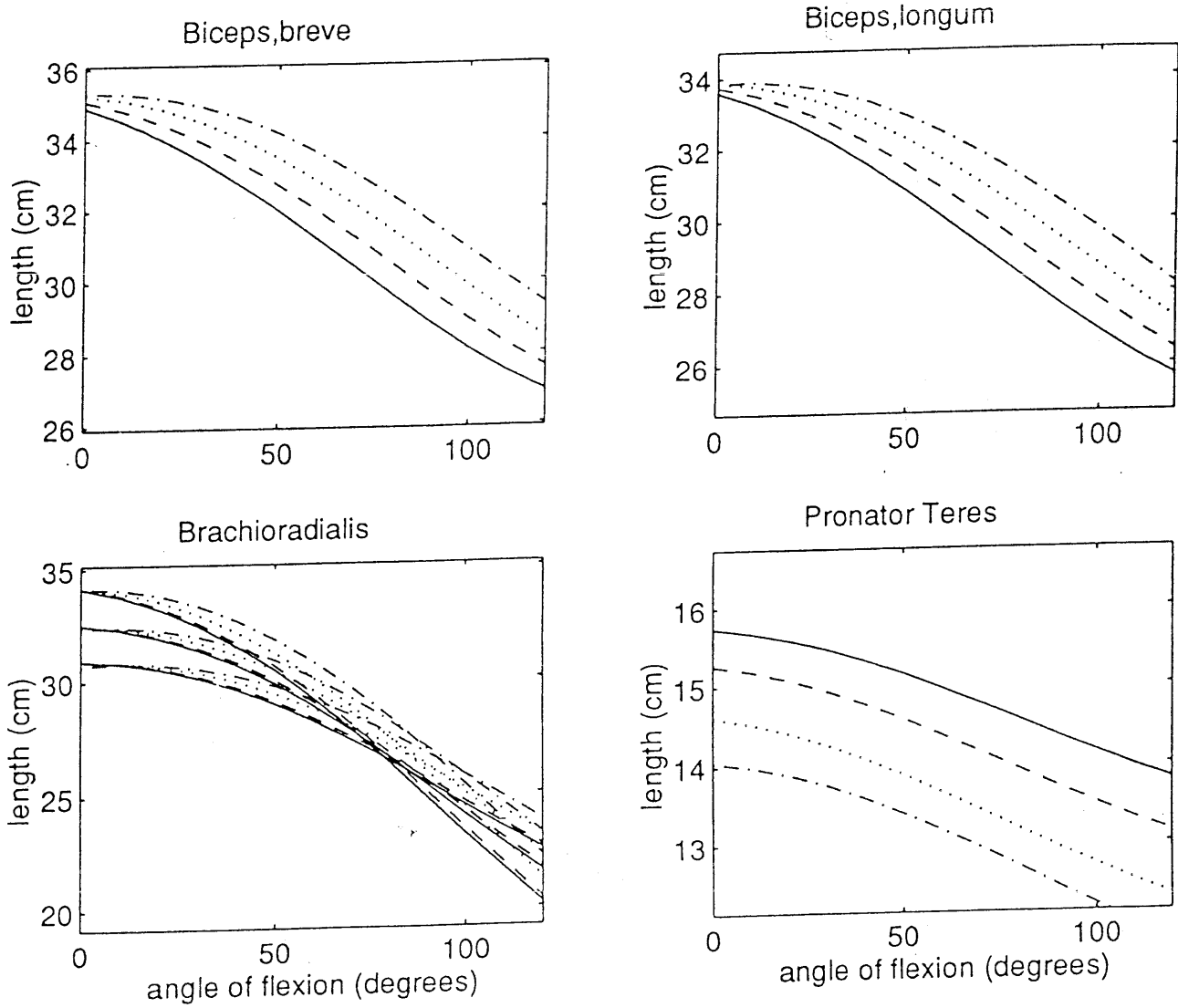


Figure F1 : Effect of pronation angle on the change in length during flexion of the biceps, the brachioradialis and the pronator teres.

- 0 degrees of pronation = maximal supinated
- - - 45 degrees of pronation
- ... 90 degrees of pronation
- · - 135 degrees of pronation = maximal pronated

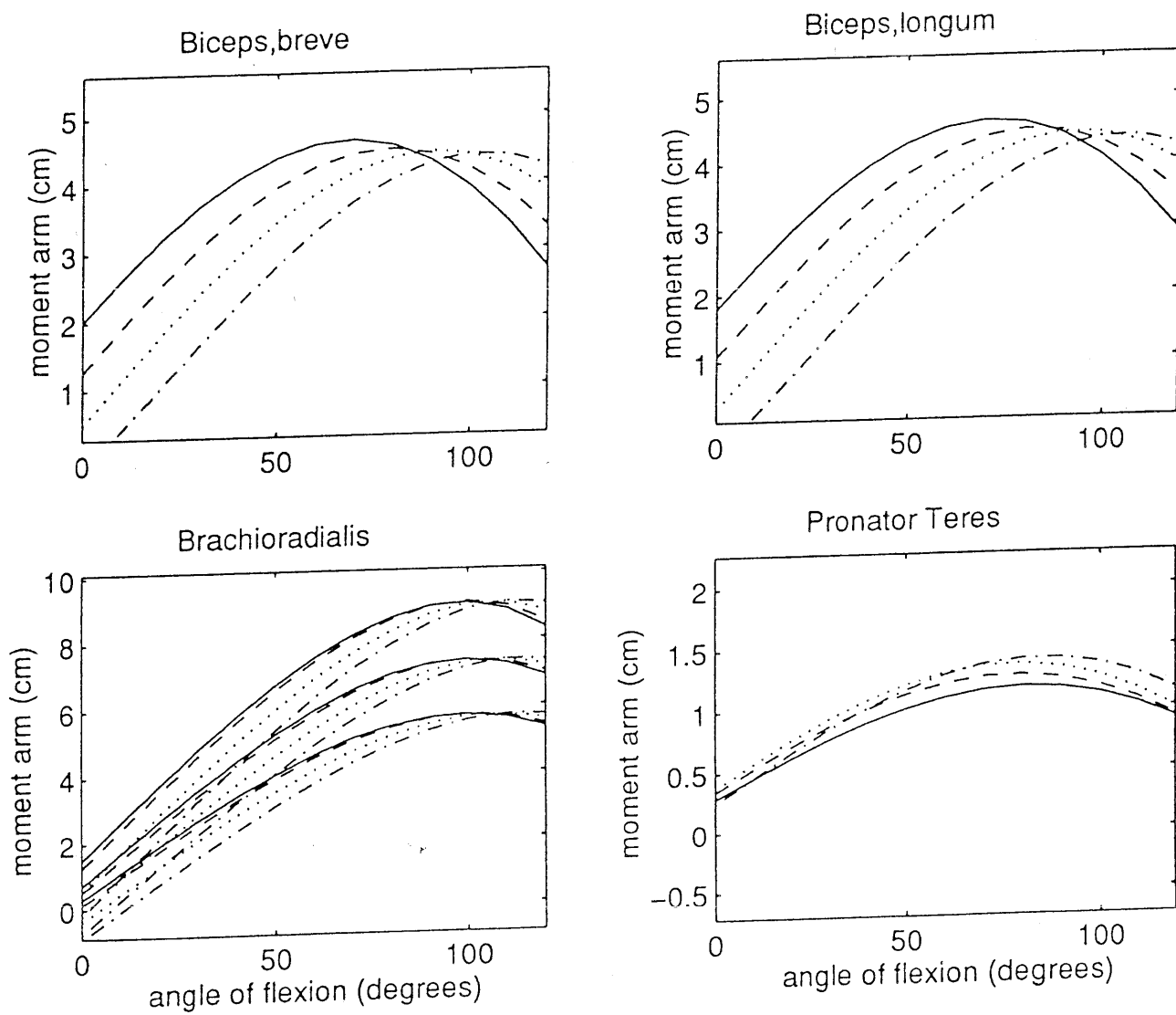


Figure F2 : Effect of pronation angle on the change in moment arm during flexion of the biceps, the brachioradialis and the pronator teres.

- 0 degrees of pronation = maximal supinated
- - - 45 degrees of pronation
- ... 90 degrees of pronation
- . - 135 degrees of pronation = maximal pronated

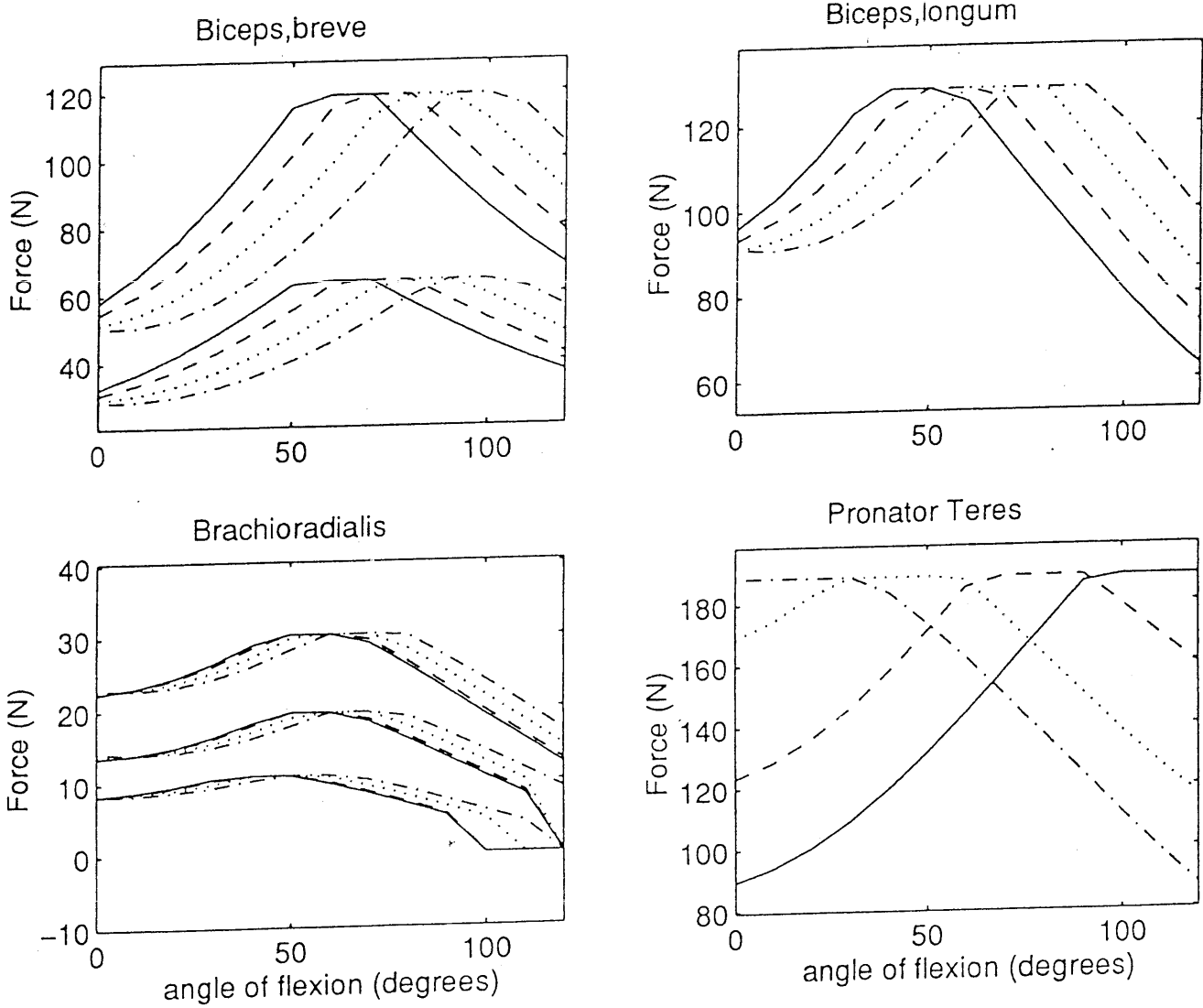


Figure F3 : Effect of pronation angle on the change in force during flexion of the biceps, the brachioradialis and the pronator teres.

- — 0 degrees of pronation = maximal supinated
- - - - 45 degrees of pronation
- . . . 90 degrees of pronation
- - . - 135 degrees of pronation = maximal pronated

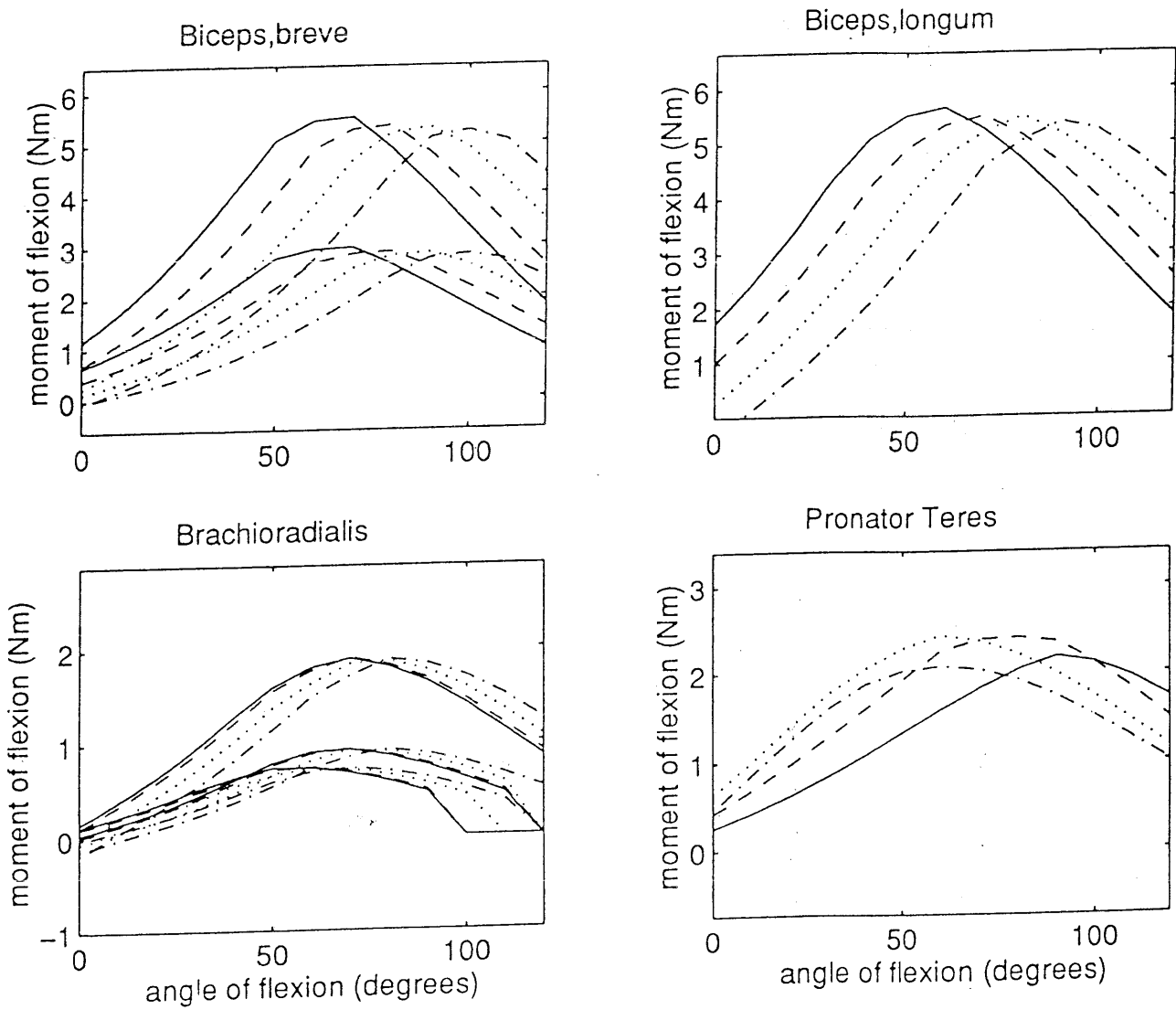


Figure F4 : Effect of pronation angle on the change in moment during flexion of the biceps, the brachioradialis and the pronator teres.

- 0 degrees of pronation = maximal supinated
- - - 45 degrees of pronation
- ... 90 degrees of pronation
- . - 135 degrees of pronation = maximal pronated

APPENDIX G : EFFECT OF FLEXION ON PRONATION

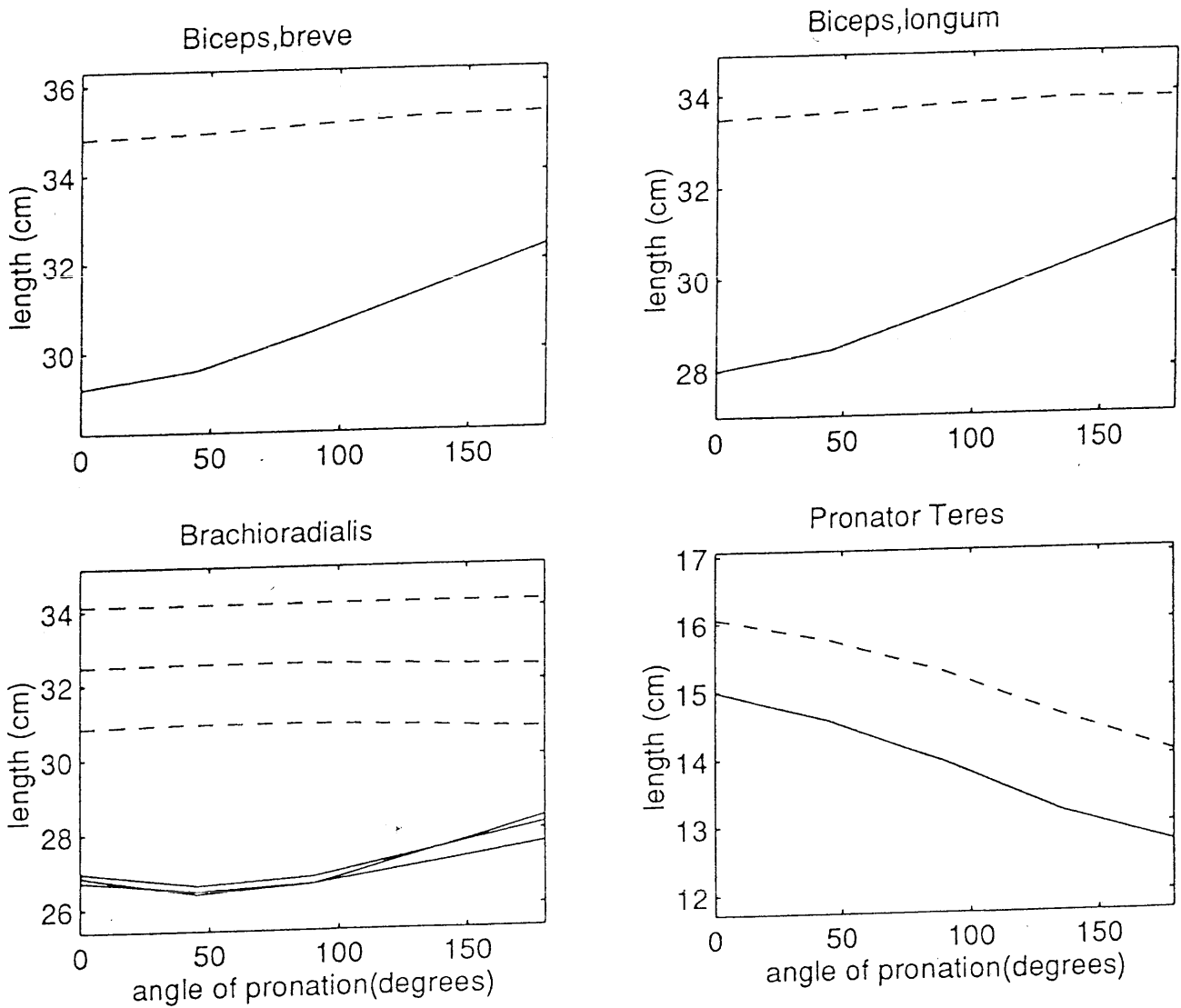


Figure G1 : Effect of flexion angle on the change in length during pronation of the biceps, the brachioradialis and the pronator teres.

- 0 degrees of flexion
- 90 degrees of flexion

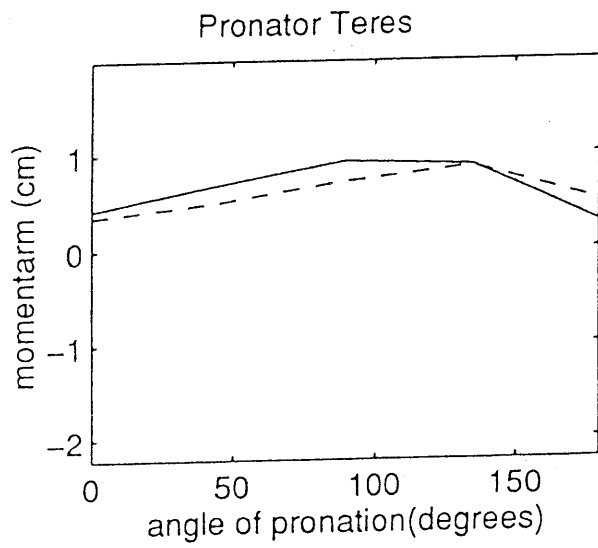
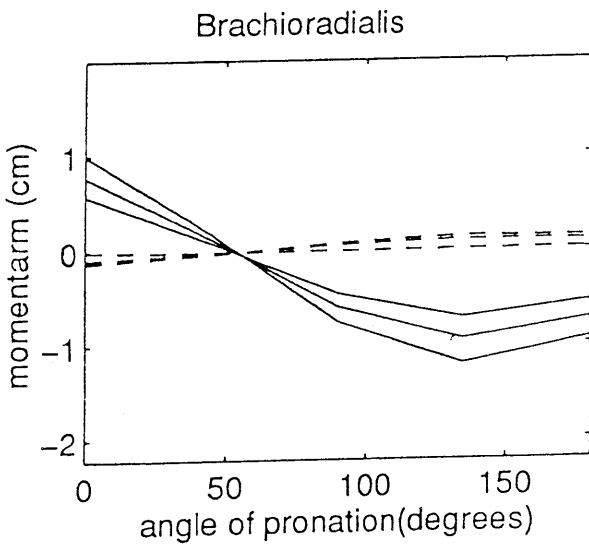
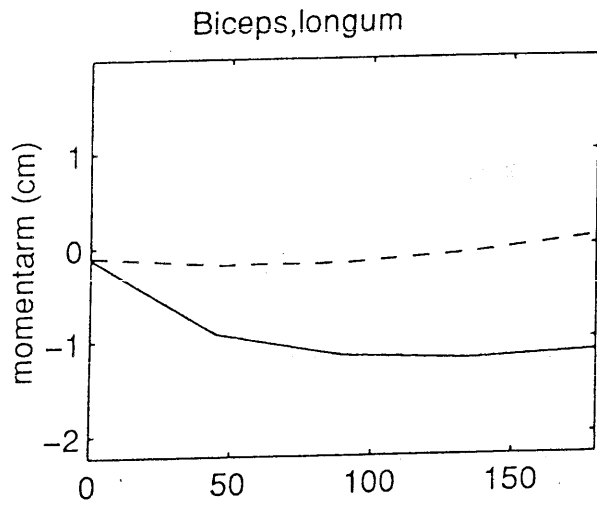
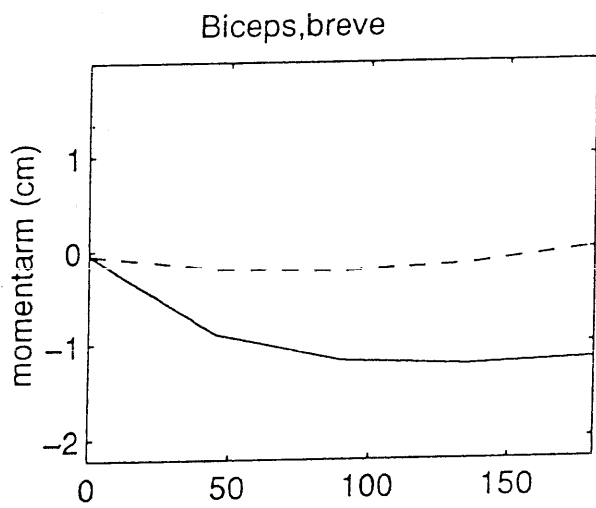


Figure G2 : Effect of flexion angle on the change in moment arm during pronation of the biceps, the brachioradialis and the pronator teres.

- 0 degrees of flexion
- 90 degrees of flexion

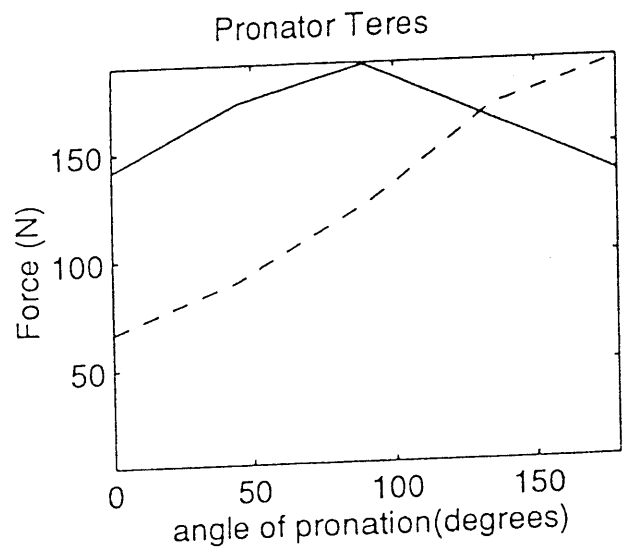
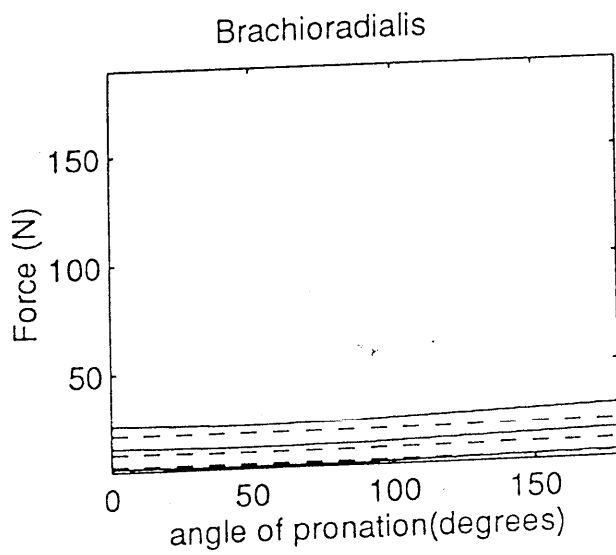
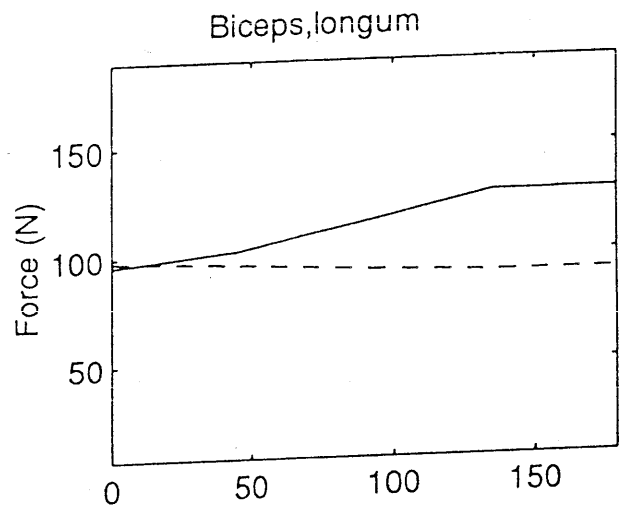
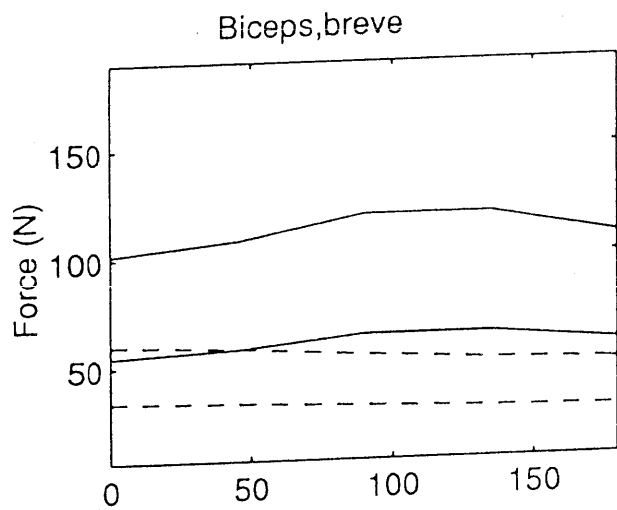


Figure G3 : Effect of flexion angle on the change in force during pronation of the biceps, the brachioradialis and the pronator teres.

---- 0 degrees of flexion
 — 90 degrees of flexion

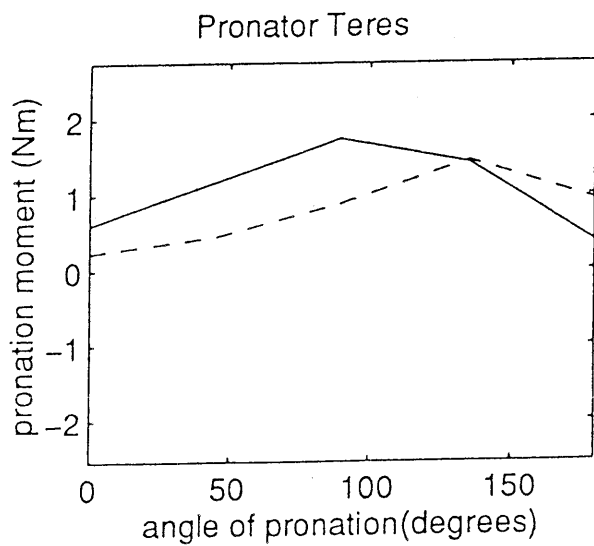
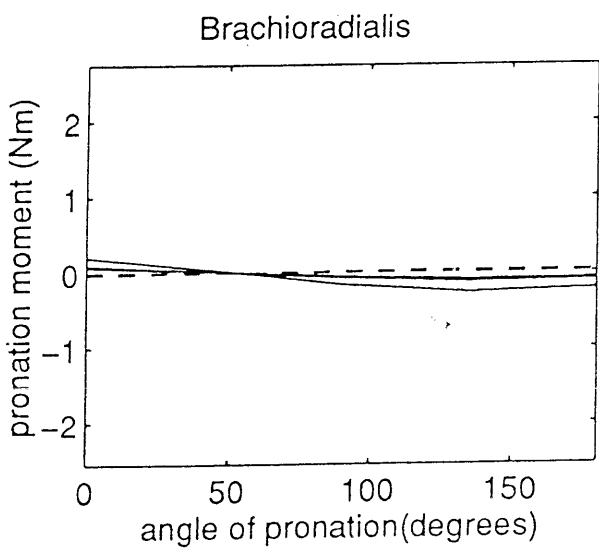
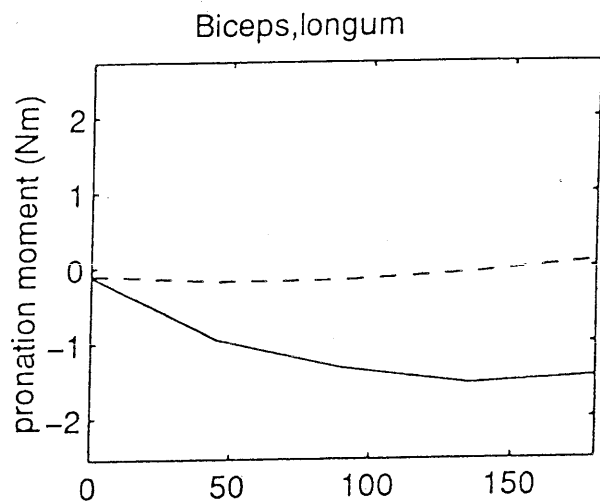
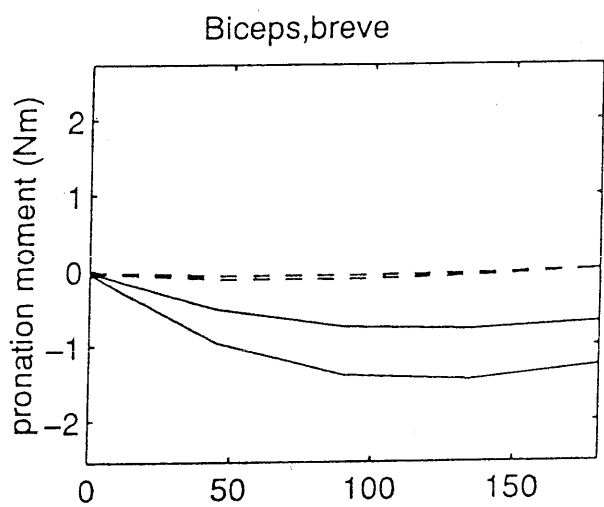


Figure G4 : Effect of flexion angle on the change in moment during pronation of the biceps, the brachioradialis and the pronator teres.

---- 0 degrees of flexion
 — 90 degrees of flexion

Table C4 : Parameters of spherical spheres

Flexion axis :
 $dx = 0.8958 \pm 0.04$
 $dy = 0.0149 \pm 0.06$
 $dz = -0.4318 \pm 0.07$

Pronation axis:
 $dx = -0.0259 \pm 0.07$
 $dy = 0.9931 \pm 0.0006$
 $dz = 0.1141 \pm 0.006$

Cylinder biceps :
 $dx = -0.1566 \pm 0.027$
 $dy = 0.9689 \pm 0.0093$
 $dz = 0.1915 \pm 0.0096$
 $X0 = 10.6243 \pm 0.426$
 $Y0 = -83.8059 \pm 6.66$
 $Z0 = 0 \pm 0.0$
 $r = 1.4118 \pm 0.019$

Cylinder brachialis :
 $dx = -0.8984 \pm 0.03$
 $dy = 0.0670 \pm 0.15$
 $dz = 0.4420 \pm 0.00$
 $X0 = 24.2067 \pm 3.0$
 $Y0 = -28.1677 \pm 1.6$
 $Z0 = 0 \pm 0.0$
 $r = 6.41957 \pm 0.9$

Cylinder pronator teres :
 $dx = -0.1032 \pm 0.011$
 $dy = 0.9602 \pm 0.124$
 $dz = 0.259 \pm 0.121$
 $X0 = 22.26 \pm 0.3$
 $Y0 = 0.0 \pm 0.0$
 $Z0 = 19.215 \pm 0.56$
 $r = 0.8794 \pm 0.34$

Cylinder supinator :
 $dx = -0.003 \pm 0.02$
 $dy = 0.97 \pm 0.003$
 $dz = 0.2083 \pm 0.021$
 $X0 = 14.22 \pm 0.8$
 $Y0 = -83.93 \pm 3.75$
 $Z0 = 0 \pm 0.0$
 $r = 1.94 \pm 0.15$

Cylinder triceps :
 Direction of the flexion axis.
 Midpoint of the elbow joint.
 The radius is estimated.

Cylinder pronator quadratus :
 Direction of the pronation axis.
 Midpoint of the pronation joint.
 The radius is estimated.

APPENDIX C

Table C3 continuation

muscle	mass (g)	vol (cm ³)	PCSA
PT hum	27.50	26.00	5.100
PT uln	4.33	4.10	1.410
SUP	0.70 0.84	0.66	0.396 0.475
	3.03 3.64	2.87	1.934 2.321
	2.80 3.36	2.65	1.052 1.262
	2.47 2.96	2.33	1.237 1.484
X	4.17	3.94	1.812
	5.63 6.76	5.33	2.377 2.852
PQ	1.63	1.54	0.726
	3.47	3.28	1.778
	4.93	4.66	2.189
TR lat	12.50	11.58	1.529
	33.20	31.39	4.097
	15.20	14.37	2.193
	16.20	15.32	2.754
	5.85	5.53	0.867
ANC	0.83	0.79	0.313
	1.50	1.42	0.704
	0.60	0.57	0.249
	2.20	2.08	1.175
	3.33	3.15	1.184

APPENDIX C

Table C3 : Muscle parameters.

vol = volume

PCSA = Physiological Cross Section Area

muscle	mass (g)	vol (cm ³)	PCSA
BIC br	20.79	19.66	1.731
	31.07	29.38	3.219
TR lg	26.97	25.50	2.229
	29.55	27.94	2.964
	29.64	28.03	2.832
	32.03	30.29	3.272
BIC lg	66.20	62.59	3.471
TR med	18.40	17.40	2.633
	17.65	16.69	2.561
	11.95	11.30	2.400
	13.95	13.19	2.113
	7.70	7.28	1.072
BRACH	29.10	27.52	3.140
	15.90	15.03	1.578
	14.65	13.85	1.572
	7.00	6.62	0.873
	6.60	6.24	1.008
	4.10	3.88	1.044
	6.50	5.15	1.181
BRD	4.70	4.44	0.296
	14.00	13.24	0.821
	5.97	5.64	0.523

APPENDIX C

Table C2 continuation

muscle	l_m (cm)	l_s (μm)	l_f (cm)	l_o (cm)	l_t (cm)	l_c (cm)
PT hum	15.233	3.560	6.722	5.098	8.511	15.74
PT uln	8.1333	3.056	3.289	2.906	4.844	9.14
SUP	4.233	2.730	1.689	1.670	2.544	4.21
	3.867 ¹	2.833	1.556	1.482	2.384	2.99
	4.033 ²	2.718	2.533	2.517	1.500	3.81
	2.1 ³	2.769	1.933	1.885	0.167	1.91
X	6.267	2.856	2.300	2.175	3.967	5.07
	3.6 ⁴	2.664	2.211	2.241	1.489	3.71
PQ	2.833	2.750	2.167	2.131	0.666	4.32
	3.300	3.108	2.122	1.843	0.178	3.65
	2.700	2.886	2.278	2.131	0.422	3.29
TR lat	23.167	2.160	6.100	7.578	17.067	22.97
	24.200	2.228	6.500	7.663	17.700	23.21
	24.367	2.050	5.256	6.556	19.667	23.72
	23.667	2.100	4.311	5.562	20.000 X	22.32
	20.867	2.120	5.167	6.383	15.700	18.72
ANC	2.633	2.133	1.989	2.517	0.644	2.73
2	3.167	2.173	1.622	2.015	1.544	2.75
3	2.333	2.533	1.900	2.277	0.433	2.40
4	6.367 *	1.983 *	1.300 *	1.797	6.033	5.32
5	4.567	2.277	2.244	2.662	2.322	4.06

APPENDIX C

Table C2 : Muscle parameters

l_m = muscle length

l_s = sarcomere length

l_f = fibre length

l_o = optimal fibre length

l_t = tendon length

l_c = length calculated by the model

muscle	l_m (cm)	l_s (μ m)	l_f (cm)	l_o (cm)	l_t (cm)	l_c (cm)
BIC br	35.400 ^{34.3}	3.500	15.176 ^{16.7}	11.700	23.333 ^{19.13}	34.86
	35.400 ^{34.3}	3.533	15.033	11.485	23.467 ^{19.24}	34.86
TR lg	28.500 ²⁷	2.167	8.400	10.468	20.100	28.25
	28.500 ^{24.5}	2.167	6.900	8.598 ^{9.75}	21.600	29.11
	28.500 ^{32.7}	2.100	7.033	9.043 ^{12.27}	21.467	29.24
	28.500 ^{32.5}	2.100	6.533	9.000 ^{13.41}	21.067	31.64
BIC lg	38.400 ^{38.5}	3.167	15.150	12.917	15.48 ^{23.35}	33.66
TR med	13.430 ¹⁵	2.056	5.033	6.608	6.397	13.75
	16.600 ¹⁸	2.228	5.378	6.518	10.222	16.28
	4.633 ^{5.5}	2.048	3.567	4.707	0.066	4.45
	8.867	2.109	4.867	6.243	4.000	8.62
	12.700	2.116	5.322	6.791	7.378	13.02
BRACH	19.167	3.42	11.100	8.763	8.067	18.89
	18.300	3.508	12.378	9.527	5.922	17.95
	15.400	3.555	11.456	8.699	3.944	14.15
	13.100	3.537	9.933	7.582	7.467	14.26
	11.267	3.537	8.111	6.191	13.156	10.70
	9.833	3.561	4.900	3.715	24.933	9.60
	9.533	3.515	6.778	5.207	12.756	9.43
BRD	38.033 ³⁴	3.161	17.567	15.005	20.466 ¹⁶	34.14
	31.000	3.187	19.033	16.127	11.967	32.51
	28.233	3.245	12.811	10.660	15.422	30.93

APPENDIX C

Table C1 continuation

ORRIGIN			INSERTION		
X	Y	Z	X	Y	Z
Pronator teres, humerus part					
14.4206	-29.3820	12.7253	17.8254	-42.4464	6.2534
Pronator teres, ulna part					
15.6018	-33.0436	11.7161	17.4898	-39.6575	7.0904
Supinator					
19.3804	-39.1150	11.7316	18.0390	-40.0887	7.0048
19.1354	-37.7749	10.8093	18.3149	-39.0238	7.4840
19.2345	-35.9683	11.4606	17.8126	-37.7083	7.7427
19.0236	-36.8253	10.9532	18.7077	-37.3396	8.57641
19.0748	-33.9830	11.4280	17.1086	-37.5295	8.4012
18.3489	-32.2621	8.8496	17.4081	-35.7479	8.8616
Pronator quadratus					
17.9056	-49.2499	9.0475	16.6466	-49.6232	5.9884
18.1215	-50.9897	8.7412	16.8887	-51.3370	6.3143
18.3957	-52.7546	8.38704	16.9574	-53.1420	6.4817
Triceps, caput laterale					
17.4217	-6.96053	9.27629	17.7566	-29.7646	13.391
17.4217	-6.96053	9.27629	17.9053	-30.0034	13.4881
17.4217	-6.96053	9.27629	18.6756	-30.5595	12.972
18.0559	-11.5231	9.75198	18.6762	-30.5593	12.9734
18.0559	-11.5231	9.75198	18.3961	-30.1639	12.9181
Anconeus					
19.405	-30.8317	11.339	18.5693	-32.5252	13.3631
19.1949	-31.2368	11.3154	18.7064	-33.2448	13.157
19.3221	-30.2857	11.4824	18.6735	-32.1559	12.9932
19.3805	-31.3437	10.6745	19.2097	-36.2926	12.6251
19.3286	-31.4166	10.9108	18.9613	-34.8441	13.0529
Extensor carpi radialis longus					
18.9251	-26.5058	11.2855	17.0495	-55.6144	4.24837
19.4061	-29.4977	10.3643	17.0495	-55.6144	4.24837
19.2822	-28.8826	10.639	17.0495	-55.6144	4.24837

APPENDIX C

APPENDIX C : Tables

Table C1 : Origin and insertion places of elbow muscles.

ORIGIN			INSERTION		
X	Y	Z	X	Y	Z
Biceps, caput breve					
13.79	-0.9974	4.768	17.8876	-35.2374	10.8931
13.79	-0.9974	4.768	17.8876	-35.2374	10.8931
Triceps, caput longum					
14.32	-4.206	11.52	17.23	-32.07	12.79
14.48	-4.074	9.657	18.23	-32.52	11.83
14.89	-3.663	10.49	18.35	-32.29	11.88
14.48	-4.074	9.657	18.59	-35.17	11.42
Biceps, caput longum, insertion part					
16.39	-1.944	5.504	17.8876	-35.2374	10.8931
Triceps, caput mediale					
16.1671	-16.5044	10.5567	17.9292	-30.1047	12.9203
16.2721	-13.9359	10.3799	17.9292	-30.1047	12.9203
18.2355	-25.5983	11.9793	17.9292	-30.1047	12.9203
17.6942	-21.3743	11.9333	17.9292	-30.1047	12.9203
16.6018	-17.0985	11.1799	17.9292	-30.1047	12.9203
Brachialis					
18.1473	-16.6056	9.6037	16.9201	-35.2391	11.3990
16.5738	-17.2617	9.1328	16.6852	-34.9737	11.7847
16.3500	-19.8392	10.052	16.2300	-33.8224	12.1896
17.1421	-20.8798	9.7196	16.9333	-34.9469	11.5242
16.3982	-23.8564	11.079	16.4500	-34.5149	12.0008
17.4124	-24.8298	10.288	16.1761	-34.0480	11.9645
16.4230	-25.3931	11.107	17.1429	-34.7633	11.2814
Brachoradialis					
17.8615	-15.6635	10.5635	15.0994	-55.3895	7.0801
18.3610	-22.3735	11.2531	15.0994	-55.3895	7.0801
18.6230	-25.0349	11.4496	15.0994	-55.3895	7.0801

APPENDIX B : INPUT FILES

In the flexion file just 5 of the 13 angles are given. These are the angles corresponding to the numbers 1-5 in figure 6 and in appendix D3. Only the flexion or pronation angle changes in these files.

AC	Acromio-claviculair y and z coordinate
TS	Trigonum Spinae x and y coordinate
AI	Angulus Inferior x and z coordinate
GHy	Abduction angle
GHz	Anteflexion angle
GHya	Endo/exorotation angle
ELx	Elbow flexion angle
PSy	Pronation angle
PO	Wrist angle x, y and z direction
HFX	Gravitation vector x, y and z direction

Flexion file

ACy	2.676	2.676	2.676	2.676	2.676
ACz	8.666	8.666	8.666	8.666	8.666
TSx	5.959	5.959	5.959	5.959	5.959
TSy	-1.069	-1.069	-1.069	-1.069	-1.069
AIx	8.683	8.683	8.683	8.683	8.683
AIz	-12.690	-12.690	-12.690	-12.690	-12.690
GHy	0.016	0.016	0.016	0.016	0.016
GHz	0.028	0.028	0.028	0.028	0.028
GHya	-0.019	-0.019	-0.019	-0.019	-0.019
ELx	0.000	0.524	1.047	1.571	2.094
PSy	0.000	0.000	0.000	0.000	0.000
POx	0.000	0.000	0.000	0.000	0.000
POy	0.000	0.000	0.000	0.000	0.000
POz	0.000	0.000	0.000	0.000	0.000
HFX	0.000	0.000	0.000	0.000	0.000
HFy	-1.000	-1.000	-1.000	-1.000	-1.000
HFz	0.000	0.000	0.000	0.000	0.000

Pronation file

ACy	2.676	2.676	2.676	2.676	2.676
ACz	8.666	8.666	8.666	8.666	8.666
TSx	5.959	5.959	5.959	5.959	5.959
TSy	-1.069	-1.069	-1.069	-1.069	-1.069
AIx	8.683	8.683	8.683	8.683	8.683
AIz	-12.690	-12.690	-12.690	-12.690	-12.690
GHy	0.016	0.016	0.016	0.016	0.016
GHz	0.028	0.028	0.028	0.028	0.028
GHya	-0.019	-0.019	-0.019	-0.019	-0.019
ELx	0.000	0.000	0.000	0.000	0.000
PSy	-0.785	0.000	0.785	1.570	2.355
POx	0.000	0.000	0.000	0.000	0.000
POy	0.000	0.000	0.000	0.000	0.000
POz	0.000	0.000	0.000	0.000	0.000
HFX	0.000	0.000	0.000	0.000	0.000
HFy	-1.000	-1.000	-1.000	-1.000	-1.000
HFz	0.000	0.000	0.000	0.000	0.000